Art Analysis & Research

ANALYTICAL REPORT

[Ref.: AAR0955.I / 8 May 2018]

Nature morte à l'écrevisse (Still Life with Crayfish), c. 1907
Mikhail Larionov
Collection Museum Ludwig, Cologne, Inv. Nr. ML 1331

Art Analysis & Research Inc.
Ground Floor West, 162-164 Abbey Street, London SE1 2AN
T: +44 (0) 20 7064 1433
VAT Reg. No. 252 4541 22

Art Analysis & Research

Summary

A painting on canvas by Mikhail Larionov, *Nature morte à l'écrevisse (Still Life with Crayfish)*, belonging to the Museum Ludwig (reference: ML 1331), that has been dated to 1907 (it is undated, and inscribed 'M[L]' in Cyrillic), was examined and analysed by Art Analysis & Research, Ltd. in cooperation with the Museum Ludwig, and funded through a grant from The Russian Avant Garde Research Project (RARP). This artwork formed a part of a group of fourteen well-provenanced paintings by the Russian artist couple Natalia Goncharova and Larionov, held in the collection of the Museum Ludwig that comprised the focus of this work. The goal set for this research was to investigate these paintings in order to characterise similarities and differences, with the objectives of 1) providing detailed studies of the specific paintings, 2) obtaining wider information on the artists' methods, 3) defining a blueprint for promising methodologies to develop further on other works by these artists and with an aim of applying such information in support a *catalogue raisonné*, and 4) creating the foundation for applying similar methodologies and techniques to other artists of the genre. To this end, each of the paintings are described in individual reports (as here) accompanied by a summary report under separate cover. The results of the program of examination, material analysis and technical imaging will be set out herein.

Art Analysis & Research

Contents

Tables, Figures and Plates

Art Analysis & Research

A. Introduction

The painting known as *Nature morte à l'écrevisse (Still Life with Crayfish)* (**Plate 1**) by the artist Mikhail Larionov (1881-1964), a work on canvas measuring 800 mm high by 1950 mm wide, is now part of the collection of the Museum Ludwig, Cologne (Inv. ML 1331). It is unsigned and undated; a date of c. 1907 has been proposed for its creation. It has been examined as part of a larger technical study of fourteen paintings by Natalia Goncharova and Larionov in the Museum Ludwig, as part of a project funded through a grant from the charity the Russian Avant Garde Research Project (RARP). The project goal has been to generate detailed technical profiles on authentic paintings by Goncharova and Larionov to expand the data available for art historical study and technical characterization of their work[1]; consequently, fourteen well-provenanced paintings by the Russian artist couple held in the collection of the Museum Ludwig were thoroughly examined and analysed[2]. The short-term goal of the project was to define a blueprint for promising routes of research to develop further on other works by these artists and with a long-term goal of contributing such information to support a technical *catalogue raisonné*; these recommendations are laid out in a summary report[3].

The information in this report therefore provides a detailed technical and material account of the painting. In addition, this is considered in light of the conservation history and provenance information relating to the painting, held by the Museum Ludwig; the supplementary reports produced by Verena Franken in the course of her work on the RARP project summarises this material[4]. Some of the information concerning examination of the painting has been included here, as relevant, as are a representative selection of the extensive documentation photographs she made.

The structure of this report is as follows. First, the primary findings of the visual examination and technical imaging will be described in **Section B**.

Materials analysis on micro-samples taken for pigment and binding medium identification and cross-sections is described in **Section C**.

---

[1] There is limited specific information available. This includes: Rioux, J.-P.; Aitken, G.; Duval, A. 'Étude en laboratoire des peintures de Gontcharova et Larionov', pp. 220-223. In: *Nathalie Gontcharova, Michel Larionov* [exh. cat.], Éditions du Centre Pompidou : Paris (1995). Rioux, J.-P.; Aitken, G.; Duval, A. 'Matériaux et techniques des peintures de Nathalie S. Gontcharova et Michel F. Larionov du Musée national d'art moderne', *Techne* **8** (1998) 7-32. Gallone, A. 'Œuvres de Michel Larionov et Nathalie Gontcharova: Analyse de la Couleur', *Le dessin sous-jacent la technologie dans la peinture: Colloque XI 14-16 septembre 1995*, R. Van Schoute and H. Verougstraete (eds), Louvain-la-Neuve (1997) pp. 137-141, Pl. 74-76.

[2] These include: Natalia Goncharova: *Paysage de Tiraspol (Tiraspol Landscape)*, 1905, ML 01483; *Rusalka*, 1908, ML 1304; *Still Life with Tiger Skin*, 1908, ML 1305; *The Jewish Family*, 1912, ML 1369; *The Orange Seller*, 1916, ML 1484; *Portrait of Larionov*, 1913, ML 1319.
Mikhail Larionov, *Still Life with Coffee Pot*, c. 1906, ML 01486; *Still Life*, c. 1907/1912, ML 1487; *Still Life with Crayfish (Nature morte à l'écrevisse*), c. 1907, ML 1331; *Portrait of a Man (Anton Beswal)*, c. 1910, ML 1306; *Rayonism, Red and Blue (Beach)*, 1911, ML 1333; *Saucission et maquereau rayonnists (Rayonistic Sausage and Mackerel)*, 1912, ML 1307; *Venus*, 1912, ML 1332; *Rayonistic Composition*, inscribed 1916, ML/Z 211/134.

[3] *Summary Report of the RARP Goncharova/Larionov Project, with the Museum Ludwig*, Art Analysis & Research Inc. (2017).

[4] See reports: *AAR0955.I ML 1331 Conservation*, Franken, V. 'Report on the examination of the painting *Still Life with Crayfish* by Mikhail Larionov' (2017a) and *AAR0955.I ML 1331 Archives*, Franken, V. 'Report on the content of the Museum Ludwig archives, concerning the painting *Still Life with Crayfish* (1907) by Mikhail Larionov' (2017b).

Inferences drawn regarding the painting on the basis of these investigations will be discussed in **Section D**.

The methodologies and protocols used in each case may be found described in the general **Protocols** supplement, appended to this series of reports.

B. Examination, imaging and analysis of the images

B.1 Methodology

The painting was initially examined visually under normal lighting conditions and with ultraviolet light (UV), then with a stereo binocular microscope.

A range of technical imaging techniques were also employed (**Appendix 3**), generating a variety of images and imaging datasets[5]. These are presented as follows:

- High-resolution visible colour (**Plates 1, 5**);
- UV luminescence (**Plates 2, 6**);
- Oblique illumination (**Plate 3**);
- 3D laser surface scanning (**Plate 4**);
- Short-wave infrared (SWIR), 1600-2500nm (**Plates 7, 8**);
- X-radiography (**Plates 9, 10**).

Additionally, weave analysis (including thread counting) was conducted on the basis of the X-radiograph (**Plate 11**). Some exemplar images recorded as part of the surface microscopy and macrophotography are also reproduced here (**Plates 12-17**).

The imaging revealed a range of aspects regarding the use of materials, structure and technique of production of the painting that are complementary to the visual observations made. Consequently, specific observation will be made to each in this section regarding the interpretation of these specific forms of analysis, while a summary overview in the context of the painting technique is presented in **Section D**, below.

B.2 General observations

The painting is executed on canvas, which has not been lined, so that both the recto and the verso of the artwork could be studied. The painting is double sided; an unfinished composition, painted over with a thin layer of white, is found on the verso. Consequently, the subject matter of this composition is unclear, and it appears to be unfinished. The painting is not on its original stretcher, having been restretched onto a newer, secondary support. Though the paint and ground are

[5] Additionally, a visible-NIR multispectral dataset was collected to examine its suitability for study of paintings of Goncharova and Larionov. This has not been otherwise reproduced or further analysed here but is available for study in the future.

somewhat brittle, the painting is in good condition, with localised consolidation and retouching where there have been small losses of paint, particularly along the edges. The paint and ground are somewhat matte, suggesting a low concentration of binding medium, and are subsequently quite brittle. There is extensive, brittle cracking of the thicker paint layers and some areas have been somewhat abraded and slightly soiled.

B.3 Imaging

Each form of imaging offers different types of insight into the various material aspects of the painting. The most relevant are introduced, in brief, here.

B.3.i Photography with ultraviolet illumination

Excitation by ultraviolet (UV) light can induce luminescence[6] in some materials, commonly seen as a weak re-emission of light in the visible region. Many natural varnishes have this property, emitting a characteristic weak greenish luminescence. While some pigments (notably zinc white and certain 'lake' pigments) are also active in this way, paints otherwise often do not luminesce. Because of the luminescence of varnishes, which are typically applied as a continuous coating across the surface of a painting, this can provide a means of determining if any disturbance has occurred, such as partial cleaning of the surface or addition of later restoration, where the changes show in contrast to the luminescent areas. Consequently, UV light is commonly used to reveal the presence of retouching. When paintings are not varnished, as is the case here, differences between the colour of the luminescence of the different paints and any added retouching paints can also indicate later stages of intervention (as here; **Protocol 3.2** and **Plate 2**).

In the UV image of this work, retouching is readily distinguished as it appears dark. Of the original paints, only those containing zinc white exhibit a distinct luminescence; the areas of more or less pure white are a dull yellow in tone.

The same may be said for the verso of the canvas.

B.3.ii Surface conformation

Two techniques for examination of the surface structure of the painting were used: photography under oblique illumination (**Plate 3**) and 3D laser scanning (**Plate 4**). While the former may be the more familiar of the two as a physical examination technique, both essentially provide a means of elucidating paint texture and object deformations, either by recording shadowing, or through direct measurement of surface height. Of the two, 3D laser scanning offers important advantages in terms of being more replicable in the future (to support longer-term conservation assessments for example) and as a numerical dataset that

[6] Commonly referred to as 'UV fluorescence', the word *luminescence* is used here as a broader term that may encompass not only fluorescence phenomena (prompt re-emission of light), but also phosphorescence (slow re-emission of light due to transition via forbidden quantum states). In both cases emission is typically at longer wavelengths than the excitation; here, the excitation is in the UV to blue part of the spectrum (hence 'UV'; in practice, so-called UV-A) and emission in the visible region.

can be studied visually and algorithmically for diagnostic features of technique. Imaging of the painting using oblique illumination, as well as 3D laser surface scanning (see **Protocol 3.3**), served to reveal two kinds of textural features that are particularly evident in this painting. The most visually dominant is the narrow, vertical cracking that is especially prominent in the most thickly painted area, though generally visible overall.

A comparison between the 3D image and the X-ray (**Plate 10.a**) is instructive in this regard; the X-ray reveals the highly pronounced cracking, and its relation to the paint thickness (**Plate 10**).

Impasto arising from the brushwork is indicative of a fluid application of paint, with distinct build-up along edges of colour areas.

B.3.iii Short-wave infrared (SWIR)

The interest in technologies capable of imaging artworks past the red end of the visible spectrum, in the 'near' ('NIR') or short-wave ('SWIR') infrared regions, has primarily developed out of the long-standing application to reflectography, exploiting the phenomenon of variable transparency of paint films at different wavelengths to enable visualisation of features lying beneath the surface. Imaging of underdrawing has been a major contribution to the study of authorship in paintings, permitting a fuller comprehension of artists' working practices and extending the evidence used in attribution questions. Practical experience (as well as theoretical consideration) has shown that deeper IR cameras can confer additional benefits in terms of penetration to underlying layers; consequently, a system capable of operating in the SWIR region was used here (see **Protocol 3.4**).

In the IR image (**Plates 7-8**), no discrete underdrawing can be resolved. However, examination of the canvas under magnification reveals the clear presence of a powdery, black-grey material, which clearly does relate to the process of setting in the composition (see **Plates 15.c, 16.a, 16.b**, with indications of observed passages of underdrawing). There also appears to be use of a thin, dilute paint used as a second stage of the laying in of the composition; such markings are likewise visible in the detailed images. The reason for the lack of resolution in IR lies in a number of factors, probably a combination of the thin and diffuse distribution of the material and the IR blocking properties of the thick overlying layers of paint.

B.3.iv X-radiography and weave analysis

X-radiography shows internal structures in paintings because the transmitted X-rays are blocked to different degrees by virtue of the inherent absorption and thickness variations of the constituent materials. For example, pigments based on lead (such as 'lead white', as here) stop the passage of X-rays more effectively than materials based on organic compounds (such as carbon blacks or the binding medium of the paint), while a thicker application of a material will block more than a thinner one. This allows visualisation of sub-surface features, such as abandoned or altered earlier phases (*pentimenti*), use of techniques such as superimposed forms as opposed to forms left in reserve, characteristic brushwork and so forth.

Here, the prepared surface of the canvas is mostly heavily covered by the application of paint but as shapes are painted in reserve, areas in between forms are often only thinly coated or left exposed. Consequently, the X-ray (**Protocol 3.6**; **Plates 9, 10**) reveals a very direct rendition of form, with thickly painted areas imaging brightly (where they block the passage of X-ray energy) and dark linear shapes surrounding many of these forms. The dark areas corresponding to the thinly primed areas of canvas that were left visible (that is, unpainted; these are more X-ray transparent than heavily worked regions). The paint seems to have been applied following a carefully determined plan – apart from the glass bottles, which are supposed to be somewhat transparent, there is no evidence of overlap, and no *pentimenti*.

Infilling of the interstices of the threads comprising the canvas support with the priming (ground) and paint also allows the canvas weave to be visualised in the X-ray (without the presence of the paint and lead containing ground, the carbon-based canvas would not be resolved by the X-ray). Even if a painting is lined, making direct access to the original canvas difficult or impossible, X-ray images can permit the primary weave structure to be examined in detail. A common characterisation of canvases (apart from weave type) cited in the study of paintings is the 'thread count', or number of threads per unit in warp and weft directions. Conventionally determined by hand-measuring a number of representative areas, this is now done by applying an image processing algorithm to the entire X-ray image, which has the benefit of providing both greatly enhanced determination of thread counts as well as density and thread orientation information across the whole painting (see **Protocol 3.7**; **Plate 11**).

The thread count on this work was determined 14.7 threads per cm in the warp (horizontal) direction and 14.4 threads per cm in the weft (vertical) direction. The well-distributed and even cusping distortion around the side edges of the canvas suggests that the painting retains its original format (**Plate 11.a**).

C. Sampling and analysis

C.1 Introduction

Samples were taken of the support, ground preparation and paint layers of the work for analysis by different means in order to determine the range of materials (canvas, pigments, binders and coatings) used in the painting, the nature of the preparation layer and the sequence of layering employed in its build up.

To this end, a series of 20 locations (13 from the recto, 7 from the verso) selected over a representative range of the painting were micro-sampled for identification of the pigments (**Tables App.1.i, App.2.i, Plates 18, 19**), with 6 micro-samples of paint taken for analysis of the binding media (**App.2.ii-2.iv**). Five further samples were taken for preparation as cross-sections (**Plates 20-28**) to study the layering in the selected areas, with the aim of elucidating the development of the painting. Finally, canvas threads were taken for fibre identification (**App.2.v**) and radiocarbon dating (**App.2.vi**).

Micro-samples for analysis were taken from locations that were adjudged to be original (that is, were clearly contiguous with those below and adjacent to them, and not retouching or repair). Locations were also further selected to represent as wide a range of the colours – and therefore probably pigments and media – as possible. Thus, the materials identified and discussed below therefore represent, as far as can be determined, the full extent of the original palette used by the artist.

The micro-samples taken for pigment characterisation were subjected to systematic analysis by polarised light microscopy (PLM) combined with UV-visible-near infrared micro-spectrophotometry, scanning electron microscopy-energy dispersive X-ray spectrometry (SEM-EDX) and Raman microscopy and some Fourier Transform Infrared Spectroscopy-Attenuated Total Reflectance (FTIR; **App.2.i-2.ii**, **Protocols 2.1-2.4**).

Organic components were identified by FTIR and subsequently by Gas Chromatography-Mass Spectrometry (GCMS; **App.2.iii**, **Protocol 2.5**). Protein staining of cross-sections using SYPRO® Ruby was also conducted (**App.2.iv, Protocol 2.6**).

All of the analytical techniques applied are standard methods within the field, capable of allowing the kinds of differentiation required for this type of work. Comparison was also made between samples from the painting and examples of similar pigments from a large collection of reference standards previously analysed by multiple means[7]. Certain differentiations cannot necessarily be made from this range of techniques, although for present purposes the level of discrimination is thought to be largely or wholly sufficient. All materials were generally identified through a combination of the techniques applied; however, certain key diagnostic features were specifically determined through one or other method.

C.2 Support

The canvas was identified as being based on linen (*Linum usitatissimum* L.) in both warp and weft directions (**App.2.iv**; **Protocol 2.7**).

C.3 Radiocarbon dating

Radiocarbon dating was applied to fibres from the canvas support (**App.2.vi**).

The radiocarbon date was determined as 121 years b.p. ±23 years. After calibration, this yielded a date distribution for which the most relevant period for the origin of the canvas lies 1903-1939 at the 95.4% probability level, pre-dating the so-called 'bomb-pulse' period that begins in the mid-1950s. Thus, the dating is compatible with the proposed dates given for the painting.

[7] The pigment reference collection belongs to the Pigmentum Project (see: http://pigmentum.org) and runs to around 3500 samples of both historical and modern origin. Analysis of this collection includes PLM and SEM-EDX as well as other techniques such as X-ray diffraction and Raman microscopy. Access to this research collection is gratefully acknowledged. Reference to specific specimens in the text of this report is to the Pigmentum collection number [Pxxxx]. An organic binding media reference collection is also held by AA&R; samples in this set are cited as [AARxxx].

C.4 Ground

The ground of the recto painting (Sample [1]) was found to be composed principally of zinc oxide, with a minor amount of calcium sulfate and traces of clay minerals (possibly also calcium carbonate). A trace of ultramarine was also identified in the sample, probably an impurity. FTIR analysis indicated that the binding medium is principally a drying oil, with the suggestion that some protein is also present. The faint irregular staining of the ground with SYPRO® Ruby would support the determination of a minor protein component is also present in the ground layer (**Table App.2.iv, Plate 24**).

The ground of the verso painting (Sample [18]) was found to be composed principally of zinc oxide with an aluminosilicate. No analysis was conducted of the binding medium.

C.5 Underdrawing

No underdrawing *per se* was identified, although there is a black underpainting and/or underdrawing. The black pigment is a carbon-based black (Sample [12]).

C.6 Paint layers: Pigments

As there are paintings recto and verso, these were both analysed. On the **recto**, the following primary pigments (**Tables App.2.i, App.2.ii**) were identified in the paint:

- Zinc oxide ('zinc white')
- Lead chromate ('chrome yellow')
- Cadmium sulfide ('cadmium yellow')
- Zinc chromate yellow
- Earth pigments, yellow and red tones, containing goethite and hematite with clay minerals
- Red lead
- Mercury(II) sulfide ('vermilion' red)
- CI Pigment Red 83:1 ('alizarin crimson')
- Chromium oxide hydrate with chromium borate ('viridian')
- Cobalt tin oxide ('cerulean blue')
- Carbon-based black, as a bone coke ('bone' or 'ivory' black)

In addition, the following compounds were identified in use as 'secondary materials' (used as fillers, brighteners, extenders):

- Lead carbonate type white ('lead white')
- Barium sulfate

On the **verso**, the following pigments were identified in the paint:

- Zinc oxide ('zinc white')
- Lead chromate ('chrome yellow')
- Earth pigments, yellow and red tones, containing goethite and hematite with clay minerals

- Mercury(II) sulfide ('vermilion' red)
- CI Pigment Red 83:1 ('alizarin crimson')
- Copper acetate arsenite ('emerald green')
- Ultramarine, synthetic, blue
- A carbon-based black, as a bone coke

C.7 Paint layers: Binding media

All samples analysed by FTIR (**App.2.ii**), including both ground and paint layers, indicated the presence of a drying oil. Additional analysis by GCMS (**App.2.iii**) on three samples indicated the presence of linseed oil in yellow and crimson red paints and poppy oil in a white. (Use of poppy oil for whites would be reasonable as it is less prone to yellowing than the other oils.)

Additionally, staining of a cross-section of Sample [17] with SYPRO® Ruby (**App.2.iv**) indicated that a yellow-grey paint probably contains a protein. However, further characterisation, such as to demonstrate the use of a mixed medium with casein, was not pursued.

FTIR (**App.2.ii**) also indicated the presence of metal soaps, probably of zinc, assumed to be reaction products between pigments and binding medium.

C.8 Stratigraphy

The preparation of cross-sections allowed for examination of the overall stratigraphy and composition of the priming and paint layers. In this case, since there are both recto and verso compositions, there are two separate structures. Additionally, there has been some penetration through the canvas of the verso ground to the recto face.

From the recto, Samples [14] (**Plate 20**), [15] (**Plates 21, 22**), [17] (**Plates 23-24**) illustrate the stratigraphy on that side; from the verso, Samples [22] (**Plate 26**) and [23] (**Plates 27, 28**) are correspondingly indicative.

Sample [17], a dull grey yellow from the recto, shows an initial white ground layer of which the lower part includes particles with the green luminescence characteristic of zinc white, indicating a double-layer structure. The probable interpretation here is that the zinc white-containing phase is actually ground that has penetrated through from the verso preparation, with the overlying layer also containing zinc white but with far fewer luminescent particles visible. This interpretation is supported by comparison to the two other samples from the recto and the two samples from the verso; in the latter (Samples [22. 23]), the more zinc white-rich ground is visible immediately below the subsequent paint layers, while in the former (notably Sample [14], which has more ground present) only the less zinc white-rich stratum is present.

An inhomogeneous green layer lies on top of the ground in Sample [17], with a darker green streak at the base, and also streaks of pink. The yellow-brown layer includes black, red and green particles and has a light green patch in one area, probably paint from the layer below. This sample seems also to contain particles of the underdrawing material on the ground, mixed in with the paint.

Sample [22], a brown from the verso, shows a white ground covered with a pale pink layer including fine red particles and a few blue particles. Both layers contain many UV-luminescent particles with the characteristic appearance of zinc white. The uppermost orange-brown layer has orange-red, brown and colourless particles.

D. Discussion of the findings

D.1 Support, ground and preparatory work

D.1.i The support

The painting has been executed on a medium weight, plain-weave linen canvas (**Plates 14.a, 14.b, 14.c**), with thread counts of 14.7 threads per cm in the warp (horizontal in terms of present orientation to the composition) direction and 14.4 threads per cm in the weft (vertical) direction (see **Plate 11.d**). The threads exhibit a z-twist. A selvedge is preserved along the lower edge, allowing the orientation of the warp and weft to be unambiguously determined (**Plate 14.b**). The weave is of medium density and relatively uniform aspect; not exactly tight, but with only small gaps between the threads (**Plates 14.b, 14.c**). While some slubby and irregular threads may be noted, they are neither very numerous, nor much thicker than the other threads (**Plate 17.b**).

The canvas is unlined, so the verso is fully visible (**Plates 5, 6**). It is affixed to a non-original stretcher (with keys at each corner and both horizontal and vertical support bars). The members of the stretcher measures c. 60 mm in width. The tacking margins generally extend over the edge of the strainer, overlapping slightly to the verso (**Plate 5**).

There are a number of inscriptions, stamps and labels present on the verso of the painting (both stretcher and canvas) that are less directly related to the original creation of the artwork (**Plates 5, 6**)[8].

D.1.ii Priming

The history of the painting begins at the verso, which was primed and used before the work was abandoned, unfinished. The reverse of the canvas that work canvas has been primed with a white ground layer based on zinc white (with a very small component of clay minerals, aluminosilicates) that is typical of Larionov and Goncharova's practice in the pre-Paris years. While it cannot be ascertained that the ground was applied by hand, it is assumed so, given the material context of other works, and also, the fact that in some areas the paint appears to extend to the cut edges of the canvas (**Plate 17.c**). The medium of this ground was not analysed.

In cross-section (**Plates 26-28**) it can be noted that the ground contains a large quantity of particles of zinc oxide that exhibit a very bright green luminescence. In comparison, the

[8] These are described in more detail in V. Franken, *AAR0955.I 1331 Conservation Report* (2017a).

priming on the recto includes very few particles of this character. This difference allows us to ascertain that the priming of the verso likely penetrated to some degree to what is now the recto of the canvas (as seen in many other of Larionov and Goncharova's works that have been studied); the irregular lower strata observed in Sample [17] (**Plates 23, 25**) gives evidence of this.

The ground of the recto painting (Sample [1]) was found to be composed principally of zinc oxide, with a minor amount of calcium sulfate and traces of clay minerals (possibly also calcium carbonate). A trace of ultramarine was also identified in the sample, probably an impurity in the sample, as it is not evident in the cross-sections prepared (**Plates 20-25**). In cross-section, the layer may be seen to luminesce a homogeneous dull greenish-beige tone; although an occasional brightly luminescent particle may be seen on occasion, there are very few of them, in contrast to the ground on the verso.

FTIR analysis indicated that the binding medium of the ground of the recto is a drying oil. It was clear hand applied after the painting was stretched; brush marks are visible in some areas of the exposed ground (**Plates 15.b, 16.a**) and the priming extends only to the turnover edge (or slightly before) or slightly further (**Plates 13, 14.a, 14.b**). However, a thin layer of protein-based (traditionally glue) sealant may have been used, or, the canvas may have been treated with a proteinaceous material as part of the production process (a 'stiffener').

Seen at magnification, the ground is shown to be quite covering; the fibres of the threads of the canvas are well covered, and the surface masks the texture of the canvas to a certain degree (**Plates 15.a-16.b**). However, probably due to the various stresses set up by the reuse of the canvas, the stretching and possibly inherent mechanical weakness in the ground, the ground itself is seen to be transversed by a fine pattern of short cracks that relate to the canvas weave (**Plate 15.a**). The composition of the ground may also have contributed, as paint films based on zinc white bound in oil have been known to experience extensive cracking, often associated with early embrittlement of such paint films although the full reasons for this phenomenon are not fully clear[9]. The fact that the paint of the composition can be seen to flow into a crack in the ground (Sample [17], **Plate 23**) suggest that this cracking took place quite rapidly, as does the fact that microscopic examination of the surface shows the same phenomenon: the paint flows over the crack system in the ground (**Plates 15.a, 15.b, 15.c**).

D.1.iii Underdrawing

In the IR images taken of the painting (**Plates 7, 8**), no discrete underdrawing is resolved; this is due to the diffuse nature of the medium used, and, to the IR blocking aspect of the paints (zinc white is especially effective). Examination of the surface, however, suggests that both a dilute black paint was used to lay in forms, as well as occasional passages in charcoal (or a similar friable black medium) (**Plates 15.c, 16.a, 16.b**).

[9] Mecklenburg, M.F., Tumosa, C.S. and Erhardt, D. 'The Changing Mechanical Properties of Aging Oil Paints', *Material Research Society Symposium Proceedings* **852** (2005) pp.13-24.

D.2 Paint, pigments and binding media

D.2.i General observations

The condition of the painting is generally very good. Although the paint layers exhibit some localised cracking and flaking (the most significant along the upper edge, as may be seen in the X-ray images: **Plates 9, 10**), this has not led to significant loss of paint, and the surface structure is well preserved. The canvas appears to have sufficient tension, although some minor slackness around the edges may be observed in raking light (**Plates 3, 4**).

The painting is executed in a very sure and spontaneous manner (single strokes of paint, often applied wet-in-wet, define form in many areas). While no trace of an underdrawing was noted, given the nature of the support, the presence of preliminary work would be difficult to discern; the shapes may have been sketched with paint in advance, or roughly laid in as the artist progressed the composition. The prepared surface of the canvas is largely but not wholly covered by the application of paint, which extends but rarely over the tacking margins allowing areas of ground to remain visible in some areas of the painting (**Plates 2, 13.a**) are visible throughout the painting at the turn over edges of the canvas (mostly to the right side). No evidence for complex layering was seen; areas are worked quite directly, with mixing both on the palette, and wet-in-wet directly on the canvas (**Plate 14.c**). Airborne dirt has accumulated on the surface (**Plate 14.b**) as well as staining around the edges of the canvas. The composition has not been varnished.

D.2.ii Paint: pigment and binding medium

The palette used in this work is quite simple, consisting of many strong colours mixed to many different shades with large quantities of white ('zinc white' primarily with additions of barium sulfate and lead white). Four yellows were noted (chrome yellow, cadmium yellow, zinc chromate yellow and yellow earth), four reds (vermilion, red lead, alizarin crimson lake and red earth) with cerulean blue[10], viridian green and a bone or ivory black.

It differs considerably from the palette of the painting on the verso, which is rather more restricted – zinc white, two yellows (chrome yellow and yellow earth, two reds (vermilion and alizarin lake, ultramarine blue, emerald green – seen in clear detail in **Plate 28** – and a bone or ivory black – though due to the presence of the overlying layer of white, it was hard to be sure that all relevant tones were sampled. Reuse of a canvas by painting on the other side is not unknown in Larionov and Goncharova's *oeuvres*[11]. In this case, due to the presence of the white overpainting, it is difficult to discern the subject of the composition on the verso (**Plate 5**).

[10] Rioux, Aitken and Duval (1998) *op. cit*. p. 21 state that no cerulean blue was found in any of the works by Larionov that they examined, but that it was used by Goncharova.

[11] For example: Éditions du Centre Pompidou, *Nathalie Gontcharova, Michel Larionov* [exh. cat.], Éditions du Centre Pompidou : Paris (1995) cat. 13, p. 36 *Le salve* ; in a work of Goncharova, cat. 20, p. 48, *Portrait de Larionov et de son ordonnance.*

Analysis of the paint samples indicated that they bound with drying oils; either poppy oil, as was the case for Sample [2] a white paint (poppy is less yellowing than many other oils) or linseed oil (**App.2.iii**). The evident fluid handling of the paint, and the semi-glossy surfaces suggest the use of a medium rich paint (**Plates**). No evidence for the formation of surface air bubbles was observed, although staining (**App.2.iv, Plate**) would suggest that some of the paint contained a protein component.

The cross-sections prepared show simple layer structures with evidence of the rather heterogeneous mixing of paint as seen in other works by Larionov. Primarily, layers are quite thin, or quite thick, with only on to two discrete layers noted in any given section, consistent with the noted directness and lack of reworking that characterises Larionov's style of painting (**Plates 20-28**). In Sample [17] (**Plates 23, 25**) black particles of what may be a charcoal underdrawing are seen, scattered irregularly through the paint layers.

The painting is inscribed 'M[L]' in Cyrillic, in the lower right corner; due to localised abrasion and loss, the 'L' is only partially legible. The bluish-purple paint of the inscription has been applied to the yellow underlayer wet-in-wet, and thus appears to be contemporary with the painting.

D.2.iii Materials analysis and implications for dating

The painting has been variously dated to c. 1907-9 on stylistic grounds.

The radiocarbon measurement of the canvas gave an origin for it between 1903-39 at the 95.4% probability level, though pre-dating the so-called 'bomb-pulse' period that begins in the mid-1950s. In addition to this a period of 3-5 years typically needs to be allowed for processing into canvas and use by the artist, making 1907 roughly the earliest it could be, though suggesting a possible later dating also. An earlier possible calibrated date range of 1802-95 appears unlikely for similar reasons (that is, including a processing allowance does not make it plausible), though not wholly impossible if the canvas had been kept for longer than normal.

The materials otherwise identified in the painting would not be incompatible with the supposed date, although they also continued in use after that time and would not preclude a revision of date if deemed necessary.

The findings generally agree well with the data collected in the study of 45 paintings by Goncharova and Larionov in the collection of the Musée national d'art moderne, Paris[12]. Though some of the technical aspects noted here were not identified in that study, they are still highly plausible for the period in question[13].

[12] The ground presents the single exception, in that only grounds based on zinc white were noted in those examples prepared by the artists themselves. Rioux, Aitken and Duval (1998) *op. cit.* p. 18.

[13] The Paris research (*ibid.*) did not find any examples of grounds composed of materials other than zinc white (here lead white), or canvases composed of fibres other than pure linen (here linen and cotton). However, these are wholly period appropriate. Equally, the palette here is quite rich in the variety of pigments used and as noted, it includes cerulean blue not found in the paintings examined from the French collections.

Other technical characteristics arising from the larger review of the works of Goncharova and Larionov may also contribute to a fuller understanding of the relative dating of this painting in the future.

E. Conclusions

The examination of the painting revealed a work that was created on the other side of an abandoned composition. After the ground was hand prepared, the design was laid in, apparently with both lines in charcoal and in dilute black paint, then followed by the sure application of bright colour fields composed from a rich palette of materials, slightly different from that of the first painting. The fact that the ground is hand applied is characteristic of Larionov's practice, as is the free working of colours, often wet-in-wet. The date range of the work given, 1907-9, is wholly plausible in light of the findings.

Art Analysis & Research

F. Acknowledgements

Art Analysis & Research would like to thank the following people for their contributions:

Museum Ludwig

Dr Yilmaz Dziewior	Director, Museum Ludwig	
Rita Kestring	Deputy Director, Museum Ludwig	
Petra Mandt	Deputy Head of Conservation, Museum Ludwig	Project coordinator Paintings conservator

Project Team, AA&R

Dr Jilleen Nadolny	Principal Investigator	Project management
Dr Nicholas Eastaugh	Chief Scientist	Materials and data analysis
Bhavini Vaghji	Senior Scientist	Materials analysis
Francis Eastaugh	Senior Imaging Engineer	Scientific imaging processing
Dr Joanna Russell	Scientist	Materials analysis

Project Subcontractors

Verena Franken	Freelance paintings conservator, Cologne, Germany	Project coordinator, examination, documentation and archival research
Patrick Schwarz	Rheinisches Bildarchiv Köln, Cologne, Germany	Photographic documentation
Prof. Hans Portsteffen, Andreas Krupa	Department of Conservation, Cologne University of Applied Sciences, Germany	Capture of X-ray data
Xavier Aure-Calvet	Freelance imaging specialist, Bristol, UK	3D imaging capture and post processing
Prof Haida Liang and team	Nottingham Trent University, UK	Hyperspectral imaging
Dr Irka Hadjas and team	ETH/ Swiss Federal Institute of Technology, Zurich, Switzerland	Radiocarbon analysis

We would also like to extend our sincere thanks to the Peter and Irene Ludwig Foundation and to the RARP donors and to its board of trustees, without whose generosity and vision this project would not have been possible.

Art Analysis & Research

G. Appendices

Standard protocols used by AA&R in the preparation of this report for sampling, materials analysis and imaging are listed in each subsection below and detailed in the appendices to the global summary report.

App.1 Sampling and sample preparation

Protocols:

[P.1.1] Sampling
[P.1.2] Cross-sectional analysis

App.1.i Sampling

Table App.1.i Samples taken for analysis

#	*Colour*	*Description*	*Location*[14]	*Analysis*
1		Ground	956/260	PLM, SEM-EDX, Raman, FTIR
2		White	947/487	PLM, SEM-EDX, Raman, FTIR, GCMS
3		Yellow	176/114	PLM, SEM-EDX, Raman, FTIR, GCMS
4		Orange Brownish	226/175	PLM, SEM-EDX, Raman
5		Red Orange	407/180	PLM, SEM-EDX, Raman
6		Red Crimson	69/564	PLM, SEM-EDX, Raman, FTIR, GCMS
7		Brown	536/554	PLM, SEM-EDX, Raman
8		Blue Dark	807/191	PLM, SEM-EDX, Raman
9		Green	6/612	PLM, SEM-EDX, Raman, FTIR
10		Black	125/253	PLM, SEM-EDX, Raman, FTIR

[14] The coordinates in this column are given in millimetres, the measurements taken from the left edge of the picture, and from the lower edge of the picture.

Art Analysis & Research

Table App.1.i Samples taken for analysis

#	*Colour*	*Description*	*Location*[14]	*Analysis*
11		Blue Bright	521/495	PLM, SEM-EDX, Raman
12		Under Painting Black	479/46	PLM, SEM-EDX, Raman
13		Red Brown	144/181	PLM, SEM-EDX, Raman
14		Pink for Cross Section	956/625	CSA
15		Pale Green	956/760	CSA
16		Coating Transparent	10/438	
17		Dull Grey Yellow	0/142	CSA, SYPRO® Ruby Staining
18		Ground	Verso 770/48	PLM, SEM-EDX, Raman
19		Yellow	Verso 770/748	PLM, SEM-EDX, Raman
20		Orange Red	Verso 61/152	PLM, SEM-EDX, Raman
21		Crimson Red	Verso 785/748	PLM, SEM-EDX, Raman
22		Black Brown	Verso 585/744	PLM, SEM-EDX, Raman, CSA
23		Green	Verso 219/98	PLM, SEM-EDX, Raman, CSA
24		Blue	Verso 332/743	PLM, SEM-EDX, Raman
25		Fibre	Verso 1950/755	PLM, FTIR, C14

App.1.ii Cross-sectional analysis

Results are shown in **App.5**, **Plates 20-28**

Art Analysis & Research

App.2 Materials analysis summary results

Protocols:

[P.2.1] Polarised light microscopy (PLM)
[P.2.2] Scanning electron microscopy and energy dispersive X-ray spectrometry (SEM-EDX)
[P.2.3] Raman microscopy
[P.2.4] Fourier Transform Infrared Spectroscopy-Attenuated Total Reflectance (FTIR-ATR)
[P.2.5] Gas Chromatography Mass Spectrometry (GCMS)
[P.2.6] Cross-sectional protein staining with SYPRO® Ruby
[P.2.7] Fibre Identification
[P.2.8] Radiocarbon dating

App.2.i SEM-EDX, Raman microscopy and PLM analysis

Table App.2.i Analytical results SEM-EDX, Raman Microscopy and PLM

#	Colour	SEM-EDX (elements)			Raman Microscopy (peaks, cm^{-1})	Identification
		Major	Minor	Trace		
1	Ground	**Zn**	Al, S, Ca	*Na, Si, P, Cl, K, Ti, Fe*	**437 (vw)**	**Zinc oxide (main)** Calcium sulfate (minor) Clay minerals (trace) Ultramarine (trace impurity)
2	White	**Zn**	-	*Al, Si, S, Ca, Sr, Ba, Pb*	1439 (vw), 1297 (vw), **1049 (vw), 987 (vw), 437 (w), 380 (vw), 329 (vw),** 272 (vw), **218 (vw)**	**Zinc oxide (main)** **Barium sulfate (trace)** **Lead carbonate type white (trace)**
3	Yellow	**Zn**	Al, Cr, Pb	*Si, S, K, Ba*	**1053 (vw), 987 (vw), 971 (vw), 841 (s), 437 (vw), 403 (vw), 377 (w), 360 (m), 338 (vw), 328 (vw, sh), 138 (vw)**	**Lead chromate [P2238]** **Zinc oxide** **Lead carbonate type white** **Barium sulfate (trace)**
4	Orange-brown	**S, Cd**	-	*Al, Si, Cr, Fe, Zn, Ba, Pb*	**987 (vw), 971 (vw), 842 (m),** 545 (vw), **404 (vw), 377 (vw), 361 (w), 338 (vw), 327 (vw, sh),** 253 (vw), **141 (vw),** 121 (vw)	**Lead chromate [P2238] (trace)** **Barium sulfate (trace)** Cadmium sulfide (main)

Table App.2.i Analytical results SEM-EDX, Raman Microscopy and PLM

#	Colour	SEM-EDX (elements)			Raman Microscopy (peaks, cm^{-1})	Identification
		Major	Minor	Trace		
5	Red-orange	**Pb**	Al	*Si, S, Ca, Cr, Zn, Ba*	**549 (m), 477 (vw), 455 (vw), 391 (w), 314 (vw),** 233 (vw, sh), **224 (vw), 151 (w), 121 (vs)**	**Red lead [P0071] (main)**
					843 (vw), 549 (w), 454 (vw), 390 (w), 341 (vw), 313 (vw), 286 (vw), 253 (w), 231 (vw), **224 (vw), 151 (w), 121 (vs)**	**Red lead [P0071]** **Mercury sulfide (trace)**[15] **Lead chromate (trace)** Barium sulfate (trace)
6	Crimson red	**Zn**	Al	*Si, P, S, Cl, K, Ca, Fe, Ba, Pb*	**1480 (vw), 1327 (vw), 1292 (vw), 1188 (vw), 1161 (vw), 843 (vw), 484 (vw)**	**Pigment Red 83:1 [P1573] (minor)** Zinc oxide (main)
7	Brown	**Zn**	Al, Si, Fe	*P, S, K, Ca, Cr, Ba, Pb*	**1594 (w, br), 1314 (w, br), 843 (vw)**	**Carbon-based black** **Lead chromate (trace)** Zinc oxide (main) Iron containing earth pigments (minor) Aluminium silicate clay minerals (minor)
8	Dark blue	-	Mg, Al, Zn, Sn	*Si, S, Co*	**1594 (w, br), 1307 (w, br), 669 (w), 533 (vw)**	**Cobalt tin oxide [P0205]** **Carbon-based black** Zinc oxide
9	Green	**Zn**	S, Cr, Ba	*Mg, Al, Si, K, Ca, Sr, Sn, Pb*	-	Chromium oxide green Zinc oxide Barium sulfate
10	Black	**Zn**	P, Ca	*Mg, Al, Si, S, K, Cr, Fe, Sn, Ba, Pb*	**1594 (m, br), 1314 (m, br)**	**Carbon-based black (bone or ivory black) (minor)** Zinc oxide (main)
11	Bright blue	**Zn**	Mg, Al, Sn	*Na, Si, S, Co, Cu, Ba, Pb*	1299 (vw, br), **986 (vw), 666 (w), 529 (vw), 436 (vw), 328 (vw)**	**Cobalt tin oxide [P0205]** **Zinc oxide** **Barium sulfate (trace)**
12	Black underpaint	**Zn**	S	*Al, Si, Cl, K, Ca, Ti, Ba*	**1574 (w, br), 1305 (w, br)**	**Carbon-based black** Zinc oxide

[15] Mercury was not identified in the SEM-EDX analysis.

Table App.2.i Analytical results SEM-EDX, Raman Microscopy and PLM

#	Colour	SEM-EDX (elements)			Raman Microscopy (peaks, cm^{-1})	Identification
		Major	Minor	Trace		
13	Red-brown	**Si**	Al, Fe, Zn	*P, S, K, Ca, Cr, Sr, Cd, Ba, Pb*	**1597 (w, br), 1295 (w, br), 836 (vw), 606 (vw), 406 (vw), 293 (vw), 222 (vw)**	**Hematite** **Goethite** **Lead chromate (trace)** **Carbon-based black** Aluminium silicate clay minerals Zinc oxide (minor) Barium sulfate (trace)
18	Ground	**Zn**	Al	*Si, S, Cl*	1444 (vw), **438 (w)**	**Zinc oxide**
19	Yellow[16]	**Zn**	Na, Al, Si, S	*Mg, P, K, Ca, Cr, Fe, Cu, Ba, Pb*	**972 (vw), 842 (m), 437** (vw), 420 (vw), **404 (vw), 377 (vw), 361 (w), 342 (vw), 328 (vw, sh), 285 (vw), 254 (w), 140 (vw)**	**Lead chromate [P2238] (trace)** **Mercury sulfide (trace)**[17] **Zinc oxide (main)**
					972 (vw), 842 (s), 546 (vw), 438 (vw), 420 (vw), **404 (vw), 377 (w), 361 (m), 338 (vw), 329 (vw, sh), 254 (vw), 140** (vw)	**Lead chromate [P2238] (trace)** **Ultramarine (minor)** **Mercury sulfide (trace)**[18] **Zinc oxide (main)**
20	Orange-red	**Zn**	-	*Al, Si, S, Ca, Ba, Hg*	**437 (vw), 343 (w), 283 (vw), 253 (vs), 110 (vw)**	**Zinc oxide (main)** **Mercury sulfide [P0010] (trace)**
21	Crimson red	**Zn**	Al	*Si, P, S, Cl, K, Ca, Hg*	**1518 (vw), 1481 (vw), 1355 (vw), 1327 (vw), 1292 (vw), 1222 (vw), 1189 (vw), 1161 (vw), 843 (vw), 549 (vw), 484 (vw), 438 (vw), 343 (w), 284 (vw), 253 (vs)**	**CI Pigment Red 83:1 [P1573] (minor)** **Mercury sulfide [P0010] (trace)** **Ultramarine (trace)**[19] **Zinc oxide (main)**
22	Black and brown	-	Al, Si, Fe	*Na, Mg, P, S, Cl, K, Ca, Mn, Cu, Zn, Hg*	**1599 (vw, br), 1298 (vw, br), 393 (vw), 343 (vw), 292 (vw), 254 (m), 227 (vw), 143 (vw)**	**Mercury sulfide (trace)** **Goethite** **Hematite** **Carbon-based black** Aluminosilicate clay minerals

[16] Red, blue-green and white pigments were observed.
[17] Mercury was not identified in the SEM-EDX analysis.
[18] As noted 17, above.
[19] Sodium was not identified in the SEM-EDX analysis.

Art Analysis & Research

Table App.2.i Analytical results SEM-EDX, Raman Microscopy and PLM

#	Colour	SEM-EDX (elements)			Raman Microscopy (peaks, cm^{-1})	Identification
		Major	Minor	Trace		
23	Green	**Zn, As**	Cu	*Al, Si, P, S, Ca, Cr, Pb*	**948 (vw), 537 (vw), 493 (vw), 436 (vw), 369 (vw), 324 (vw), 286 (vw), 241 (vw), 216 (m), 171 (w), 153 (m), 120 (m)**	**Copper acetate arsenite [P1302]** Zinc oxide
24	Blue[20]	-	Na, Al, Si, S, Zn, As	*Cl, K, Ca, Cu*	**584 (w, sh), 547 (m), 257 (vw)**	**Ultramarine** Zinc oxide Copper acetate arsenite

App.2.ii Fourier Transform Infrared Spectroscopy-Attenuated Total Reflectance (FTIR-ATR)

Table App.2.ii Summary results from FTIR

#	Colour	FTIR (peaks, cm^{-1})	Identification
1	Ground	**3289 (m, br), 2954 (w), 2918 (m), 2850 (m), 1726 (s), 1645 (vw, sh), 1591 (vw), 1578 (vw), 1539 (s), 1455 (m),** 1437 (vw), **1417 (vw), 1398 (w), 1377 (vw, sh), 1317 (vw),** 1267 (vw), **1238 (vw), 1149 (m),** 1124 (vw), **1098 (vw),** 1063 (vw), 1039 (vw), 997 (vw, sh), 912 (vw), **876 (vw), 743 (vw), 721 (vw)**	**Oil** **Metal soap formation, zinc-based[21]** **Metal soap formation** **Possibly protein** **Possibly calcium carbonate, calcite type**
2	White	**3342 (w, br), 2918 (s), 2849 (m), 1734 (m), 1716 (w), 1581 (vw, sh), 1574 (vw), 1566 (vw), 1556 (vw), 1539 (vs), 1454 (vw, sh),** 1433 (vw, sh), **1406 (vs), 1318 (w), 1167 (m), 1105 (vw, sh), 1077 (s), 982 (w),** 919 (vw), **742 (vw), 723 (vw), 681 (vw), 669 (vw), 635 (vw), 609 (w)**	**Lead carbonate type white** **Barium sulfate** **Oil[22]** **Metal soap formation, zinc-based[23]** **Metal soap formation**
3	Yellow	**3348 (w, br), 2957 (w), 2918 (w), 2874 (vw), 2849 (w), 1726 (s), 1581 (vw, sh), 1574 (vw), 1567 (vw), 1557 (vw), 1539 (w), 1462 (vw, sh), 1455 (vw),** 1446 (vw), 1435 (vw), **1395 (w),** 1320 (vw), 1267 (vw), **1240 (vw), 1169 (vw, sh),** 1142 (w), **1096 (vw), 1060 (w),** 997 (w, sh), **967 (vw), 949 (vw, sh), 877 (vw, sh), 847 (vw, sh), 821 (s), 749 (vw), 721 (vw), 678 (vw), 669 (vw, sh),** 654 (vw), **625 (w)**	**Lead chromate [P2238][24]** **Oil** **Metal soap formation, zinc-based[25]** **Metal soap formation** **Possibly lead carbonate type white**

[20] Green and white pigments were observed.

[21] The peaks present in the sample spectrum matched the reference spectrum of zinc stearate, reference number AAR308. Zinc was identified in the SEM-EDX analysis.

[22] The characteristic peak of oils occurring at around 1160 cm^{-1} was not observed in the spectrum due to the presence of barium sulfate whose peaks were masking this characteristic peak of oil however it is assumed that oil is present due to the formation of metal soaps.

[23] As noted 21, above.

Table App.2.ii Summary results from FTIR

#	Colour	FTIR (peaks, cm^{-1})	Identification
6	Crimson red	**3366 (m, br), 2951 (vw, sh), 2919 (m), 2851 (m), 1732 (m), 1717 (vw, sh),** 1651 (vw, sh), **1633 (w), 1587 (s), 1575 (vw), 1567 (vw), 1556 (vw), 1549 (vw), 1539 (s), 1464 (s),** 1454 (vw), 1410 (w), **1360 (vw), 1348 (w), 1326 (vw), 1287 (w), 1267 (m), 1186 (vw, sh), 1151 (vw, sh), 1091 (vw, sh),** 1063 (vs), **1041 (vw), 1022 (w), 983 (w),** 905 (vw), 881 (vw), **839 (w), 799 (vw), 769 (vw),** 744 (vw), **719 (w), 669 (vw), 654 (vw),** 636 (vw), **609 (w)**	**CI Pigment Red 83:1 [P1573]** **Barium sulfate** **Carbonate**[26] **Oil**[27] **Metal soap formation, zinc-based**[28] **Metal soap formation**
6a	Coating	**3433 (vw, br), 2959 (m), 2933 (w), 2921 (vw, sh), 2875 (vw), 2850 (vw), 1722 (vs), 1541 (vw), 1486 (vw, sh), 1470 (m), 1449 (w, sh), 1390 (vw), 1369 (vw), 1341 (vw), 1267 (m), 1238 (m), 1172 (vw, sh), 1143 (vs), 1063 (m), 1022 (vw), 994 (m), 965 (vw), 945 (w), 910 (vw, sh), 879 (vw), 845 (vw), 801 (vw), 748 (w),** 693 (vw), 670 (vw), 654 (vw, sh), **635 (vw), 609 (vw)**	**Acrylic copolymer *pn*BMA/*pi*BMA [AAR320]** **Possibly oil from paint (traces)** **Possibly barium sulfate from paint (traces)** **Possibly metal soap formation from paint, presumably zinc-based (traces)**[29]
9	Green	**3438 (vw, sh), 3260 (w, br), 2952 (vw, sh), 2918 (w), 2849 (w), 1739 (w), 1715 (vw, sh), 1588 (w, sh), 1557 (vw), 1540 (w), 1447 (s), 1421 (w), 1362 (w), 1285 (s), 1251 (w),** 1166 (s), **1110 (vw, sh), 1067 (s), 982 (vw), 947 (m), 878 (s), 801 (s),** 714 (vw), **695 (vw), 680 (vw),** 654 (vw, sh), **632 (s), 605 (m)**	**Chromium borate**[30] **Zinc chromate [P2251]** **Barium sulfate** **Carbonate**[31] **Oil**[32] **Metal soap formation, presumably zinc-based** **Metal soap formation**

[24] The reference spectrum of lead chromate consists of peaks corresponding to lead sulfate too. These peaks are also present in the sample spectrum which could suggests that the lead chromate is likely in the form of lead chromate sulfate or lead sulfate is present in the reference spectrum too.
[25] As noted 21, above.
[26] It is not possible to say in which form the carbonate is since both lead carbonate type white and calcium carbonate show this peak. Other peaks which can be used to differentiate one from the other are absent.
[27] The characteristic peak of oils occurring at around 1160 cm^{-1} was not observed in the spectrum however it is assumed that oil is present due to the formation of metal soaps.
[28] As noted 21, above.
[29] It is assumed that the metal soap present in the sample is zinc-based since zinc oxide was present in sample 6 from which this coating was removed.
[30] The peaks assigned to chromium borate are present in the reference spectrum of chromium oxide hydrate, reference number P0092.
[31] It is not possible to say in which form the carbonate is since both lead carbonate type white and calcium carbonate show this peak. Other peaks which can be used to differentiate one from the other are absent.
[32] The characteristic peak of oil occurring at around 1160 cm^{-1} was not observed in the spectrum due to the presence of barium sulfate whose peaks were masking this characteristic peak of oil however it is assumed that oil is present due to the formation of metal soaps.

Table App.2.ii Summary results from FTIR

#	Colour	FTIR (peaks, cm^{-1})	Identification
10	Black	**3349 (w, br), 2954 (vw, sh), 2918 (w), 2849 (w), 1738 (w), 1715 (vw), 1582 (w, sh), 1539 (m), 1455 (w), 1411 (w), 1373 (vw, sh), 1317 (vw), 1242 (vw, sh), 1157 (w, sh), 1118 (vw, sh), 1026 (vs), 1015 (vw),** 982 (vw), 943 (vw, sh), **871 (vw, sh),** 798 (vw), **721 (vw), 698 (vw)**	**Carbon-based black (bone or ivory black)** **Oil** **Metal soap formation, zinc-based**[33] **Metal soap formation**

App.2.iii Gas Chromatography Mass Spectrometry (GC-MS) Analysis

Table App.2.iii Summary results from GCMS

Sample #	Hexadecanoic acid, methyl ester ($C_{17}H_{34}O_2$)		Octadecanoic acid, methyl ester ($C_{19}H_{38}O_2$)		Ratio
	Retention time, mins	Peak area	Retention time, mins	Peak area	
2	25.670	2.696×10^8	29.597	4.698×10^7	P/S = 5.74
3	25.686	5.938×10^8	29.559	6.285×10^8	P/S = 0.94
6	25.655	7.039×10^8	29.590	6.452×10^8	P/S = 1.09

The P/S value of **Sample [2]**, white paint, was 5.74, consistent with **poppy oil**.

The P/S value of **Sample [3]**, yellow paint, was 0.94, consistent with **linseed oil**.

The P/S value of **Sample [6]**, crimson red paint, was 1.09, consistent with **linseed oil**.

App.2.iv SYPRO® Ruby protein staining

Table App.2.iv SYPRO® Ruby stain results, Sample [17]

Layer	*EDX*	*FTIR*	*SYPRO® Ruby stain*	*Interpretation*
Ground	**Zn** Al *Si, S, Cl*	Oil, possible protein peak	Faint patchy pink staining of ground layer, with stronger staining of outer edge of sample at left hand side.[34]	Some minor component of protein in present in ground layer,
Paint			Clear pink staining of yellow-grey layer. Green layer appears unchanged.	Protein in yellow-grey paint

[33] As noted 21, above.

[34] The darker staining at the edges of the ground layer appears to correspond to areas at the periphery of the sample, rather than to a distinct layer at the base of the cross section. There is not sufficient evidence to identify this as a size layer.

App.2.v Fibre Identification of the Canvas

Table App.2.v Canvas fibre identification, Sample [25]

Sample	***Observations under PLM***	***Interpretation***
Weft (vertical)	Nodes across fibres, parallel extinction, s-twist. A few structures with low birefringence, some appearing as broadened ends of fibres – degraded areas?	Bast fibre, probably linen (*Linum usitatissimum* L.)
Warp (horizontal)	Nodes across fibres, parallel extinction, s-twist. One or two slender fibres with similar appearance but lower birefringence, s-twist?	Bast fibre, probably linen (*Linum usitatissimum* L.)

App.2.vi Radiocarbon measurement

Radiocarbon dating is a method for determining age estimates of formerly living organic materials[35]. Carbon has three naturally occurring isotopes, ^{12}C, ^{13}C and ^{14}C. Both ^{12}C and ^{13}C are stable, but ^{14}C decays by very weak beta decay to nitrogen (^{14}N) with a half-life of approximately 5,730 years. While alive, organic materials continue to exchange carbon with the environment, such that they are in equilibrium. On death, the ^{14}C component begins to decay, such that over time the relative amount decreases. Measuring the level of ^{14}C remaining in the material then allows for a date to be estimated. This must be additionally calibrated against natural historical variation in relative ^{14}C levels in the environment, for which there are accepted standard curves expressing the changes over time[36].

Prior to radiocarbon measurement, fibre identification was undertaken and the canvas sample was pre-tested using FTIR to ascertain the presence of any contaminating material that could influence the outcome. As noted elsewhere, the fibre was identified as a bast type, probably linen (*Linum usitatissimum* L.). FTIR indicated the presence of calcium sulfate (gypsum type), and possibly an oil, in addition to the cellulose of the fibre[37].

The canvas sample was then submitted to the Laboratory of Ion Beam Physics, ETHZ at the Swiss Federal Institute of Technology (*Eidgenössische Technische Hochschule Zürich*) for radiocarbon dating (see **Protocol 2.7**).

[35] Based on from the websites of the NDT Resource Center, http://www.ndt-ed.org/EducationResources/CommunityCollege/Radiography/Physics/carbondating.htm and the website of the Oxford Radiocarbon webinfo site: http://c14.arch.ox.ac.uk/embed.php?File=webinfo.html, both consulted on 3 February 2013.
[36] For example, that used here is one known as IntCal13.
[37] Non-cellulosic materials are aimed to be removed by the sample pre-treatment process prior to the radiocarbon measurement.

Table App.2.vi.i Radiocarbon measurement, Sample [25]

Sample-Nr.	Sample Code	Material	C14 age BP	±1σ	F14C	±1σ	δC13 ‰	±1σ	mg C	C/N
ETH-77074	AAR0955.I.25	textile	121	23	0.985	0.0028	-24.4	1	0.96	238.12

The radiocarbon date was determined as 121 years b.p. ±23 years. After calibration, this yielded a date distribution for which the most relevant period for the origin of the canvas lies 1903-1939 at the 95.4% probability level, pre-dating the so-called 'bomb-pulse' period that begins in the mid-1950s.

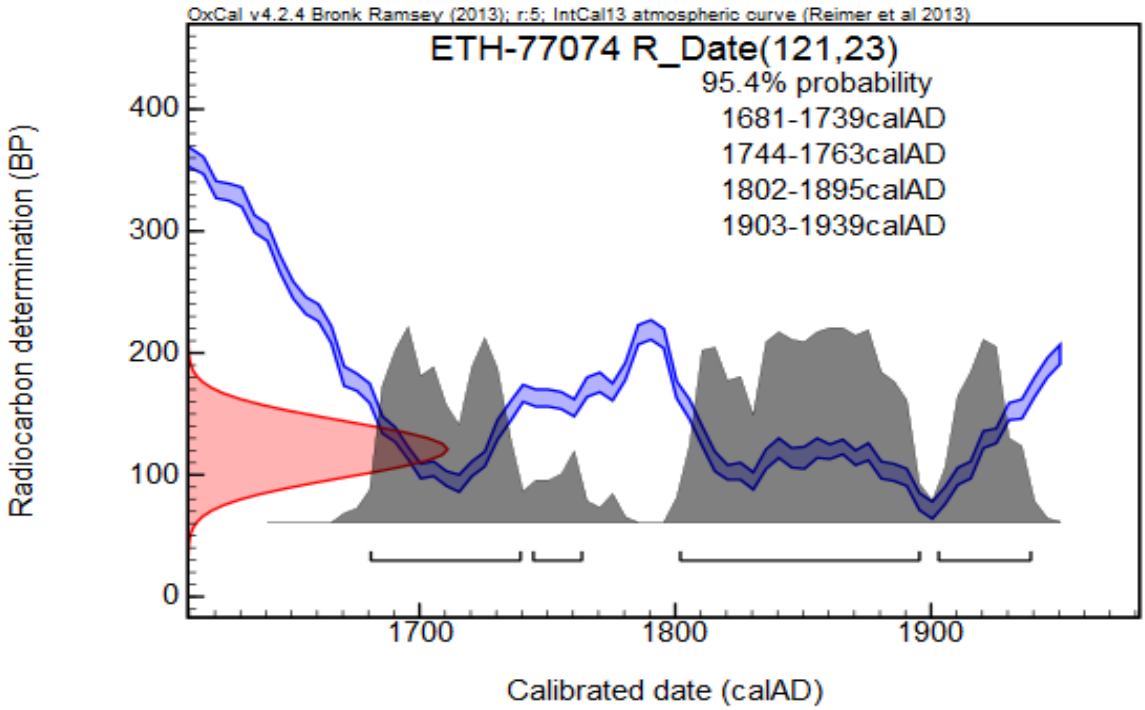

Figure App.2.vi.ii Radiocarbon determination.

Art Analysis & Research

App.3 Imaging methods

Protocols:

[P.3.1] Photography with visible light
[P.3.2] Photography with ultraviolet illumination
[P.3.3] 3D laser surface mapping
[P.3.4] SWIR infrared imaging (IR)
[P.3.6] X-radiography (X-ray)
[P.3.7] Thread counting and weave analysis

App.4 Plates

Plate 1. Mikhail Larionov, *Nature morte à l'écrevisse (Still Life with Crayfish)*, c. 1907, collection Museum Ludwig: Inv. Nr. ML 1331. **Recto, visible light.**

Rheinisches Bildarchiv Köln, Patrick Schwarz, rba_d050883_08, www.kulturelles-erbe-koeln.de/documents/obj/05020019

Plate 2. Mikhail Larionov, *Nature morte à l'écrevisse (Still Life with Crayfish*), c. 1907, collection Museum Ludwig: Inv. Nr. ML 1331. **Recto, UV light.**

Rheinisches Bildarchiv Köln, Patrick Schwarz, rba_d050883_06, www.kulturelles-erbe-koeln.de/documents/obj/05020019

The dark purple areas, readily visible along the top and bottom right edges, are retouching of localised paint loss.

Plate 3. Mikhail Larionov, *Nature morte à l'écrevisse (Still Life with Crayfish),* c. 1907, collection Museum Ludwig: Inv. Nr. ML 1331. **Recto, oblique illumination.**

Rheinisches Bildarchiv Köln, Patrick Schwarz, rba_d050883_04, www.kulturelles-erbe-koeln.de/documents/obj/05020019

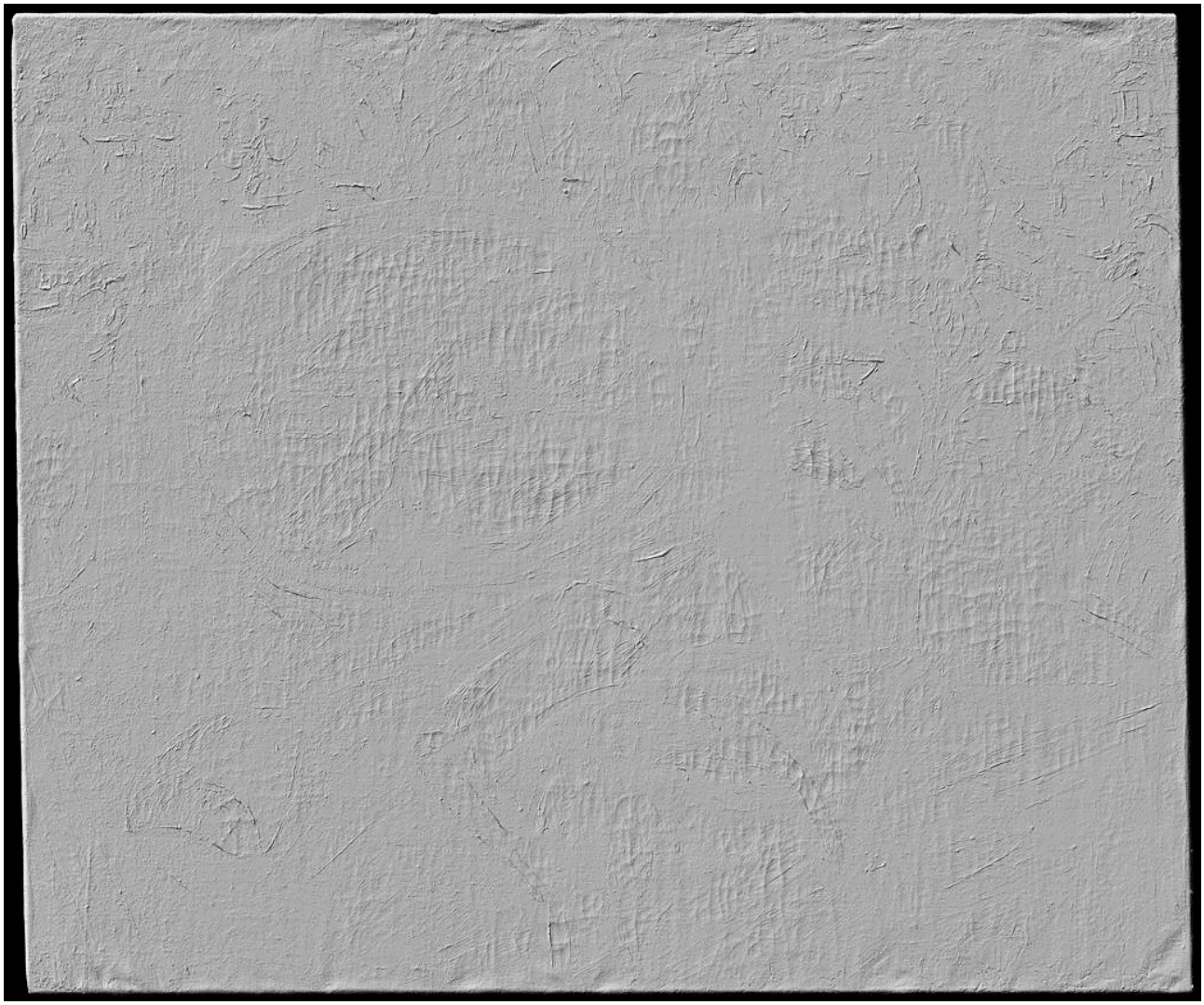

Plate 4. Mikhail Larionov, *Nature morte à l'écrevisse (Still Life with Crayfish),* c. 1907, collection Museum Ludwig: Inv. Nr. ML 1331. **Recto, 3D laser scan**.

Plate 5. Mikhail Larionov, *Nature morte à l'écrevisse (Still Life with Crayfish),* c. 1907, collection Museum Ludwig: Inv. Nr. ML 1331. **Verso, visible light.**

Rheinisches Bildarchiv Köln, Patrick Schwarz, rba_d050883_02, www.kulturelles-erbe-koeln.de/documents/obj/05020019

Below, options for orientation of the painting on the verso.


a.


b.


c.

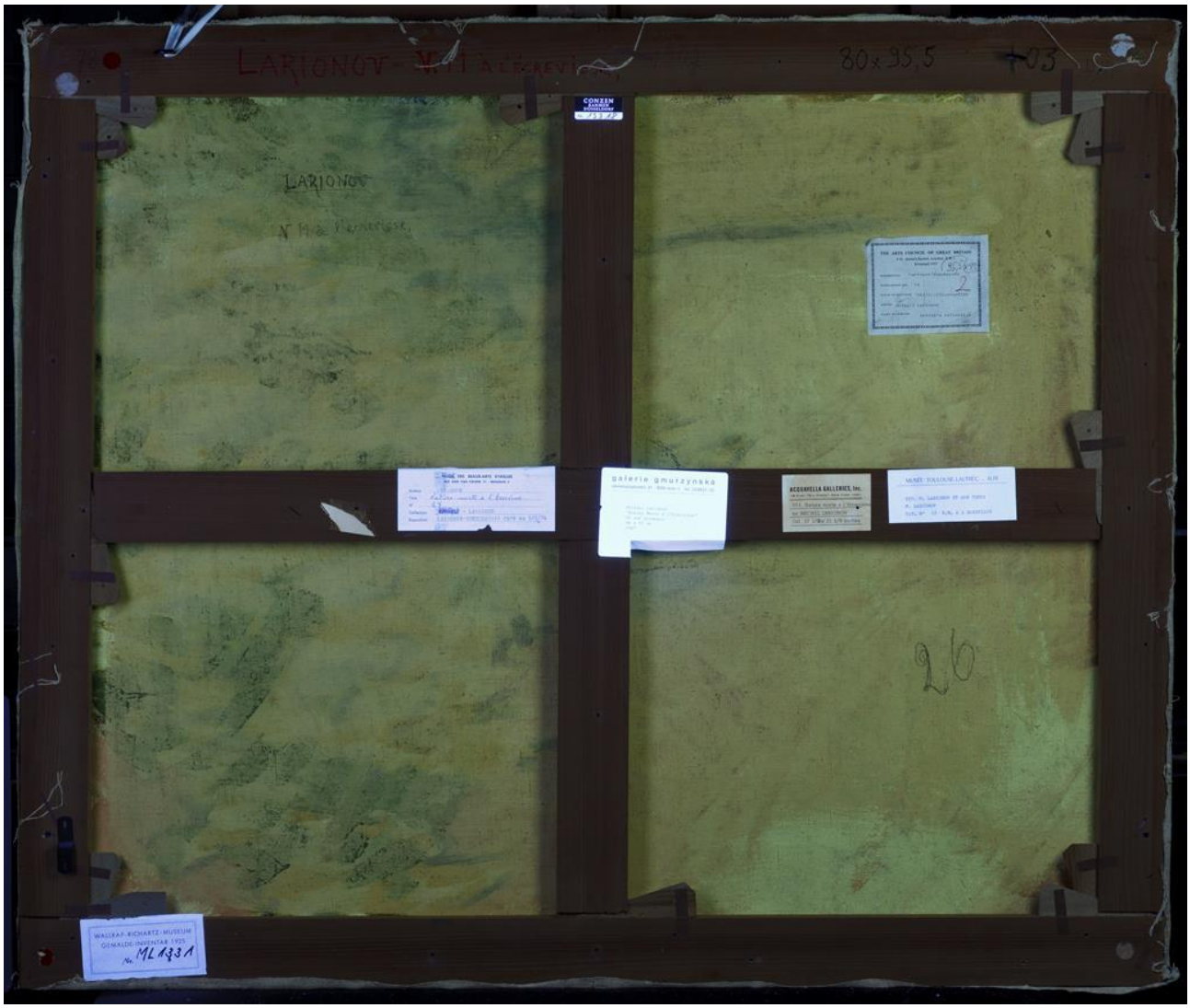

Plate 6. Mikhail Larionov, *Nature morte à l'écrevisse (Still Life with Crayfish)*, c. 1907, collection Museum Ludwig: Inv. Nr. ML 1331. **Verso, UV light.**

Rheinisches Bildarchiv Köln, Patrick Schwarz, rba_d050883_07, www.kulturelles-erbe-koeln.de/documents/obj/05020019

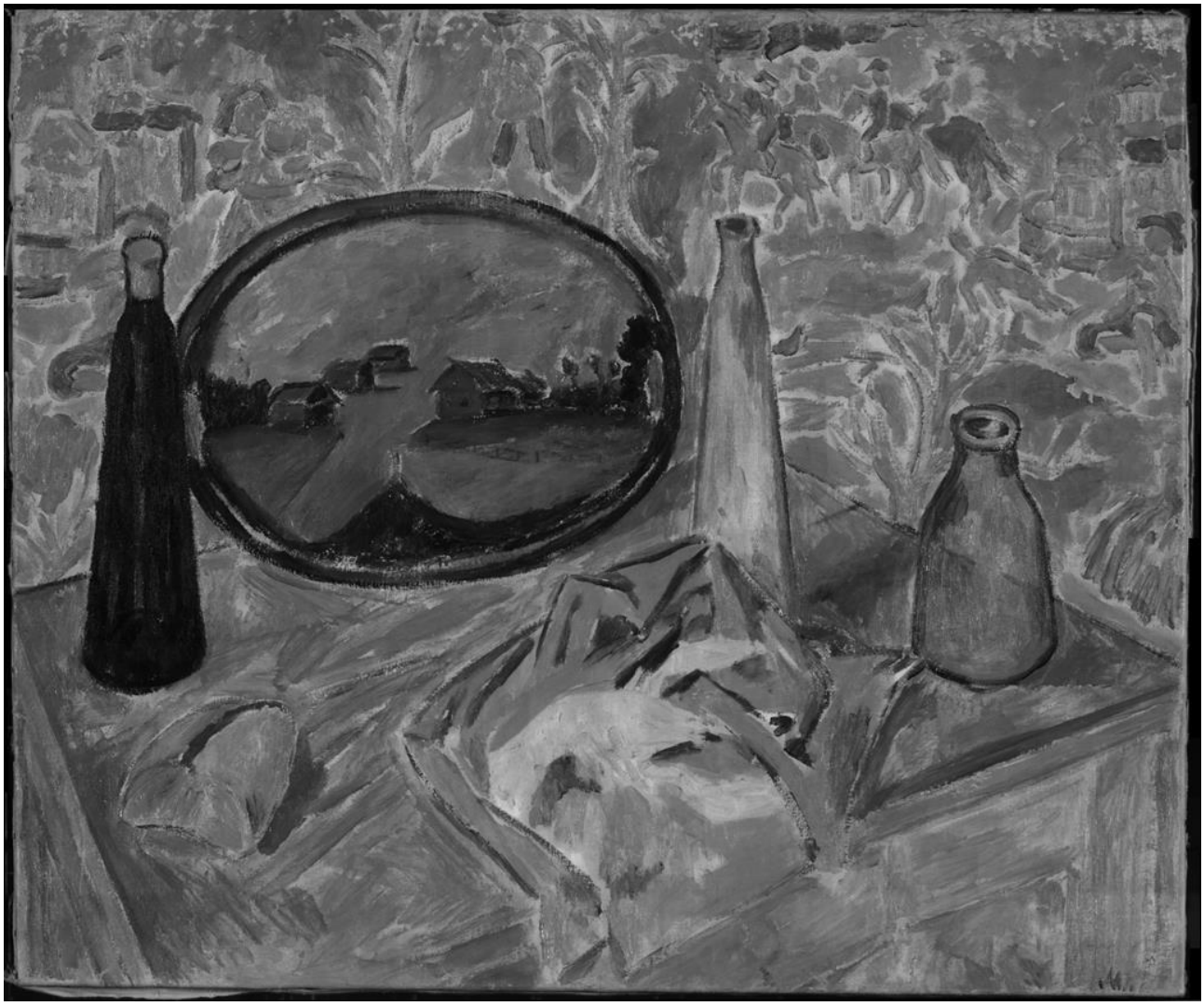

Plate 7. Mikhail Larionov, *Nature morte à l'écrevisse (Still Life with Crayfish),* c. 1907, collection Museum Ludwig: Inv. Nr. ML 1331. **Recto, SWIR image**.

Plate 8. Mikhail Larionov, *Nature morte à l'écrevisse (Still Life with Crayfish),* c. 1907, collection Museum Ludwig: Inv. Nr. ML 1331. **Recto, detail, SWIR image, upper right corner.**

No discrete underdrawing is visible, though traces of an underpainting material are visible upon examination of the artwork.

Plate 9. Mikhail Larionov, *Nature morte à l'écrevisse (Still Life with Crayfish),* c. 1907, collection Museum Ludwig: Inv. Nr. ML 1331. **X-ray image**.

Plate 9b. The X-ray image before digital compensation for the stretcher bars.

Plate 10. X-ray image, detail, upper right corner.

The direct manner in which the painting is rendered is clearly seen, though the contrast of the thick (white) brush strokes, and the primed canvas (dark) left in reserve. Flaking of the paint along the upper border (dark) is visible.

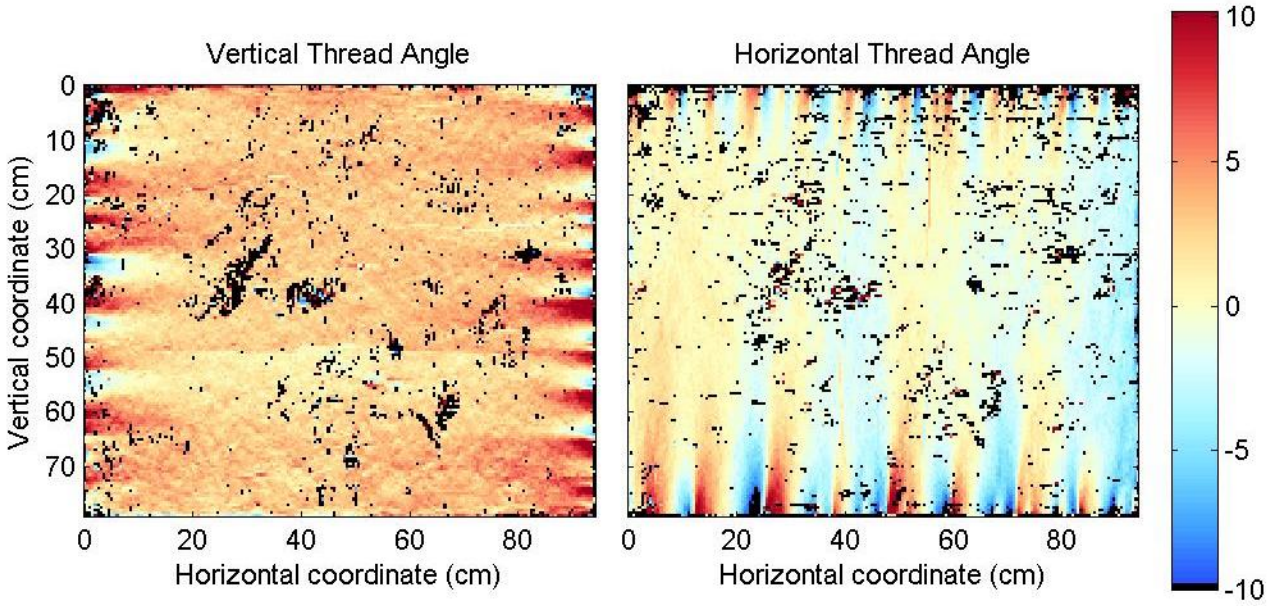

Plate 11.a Maps showing variation in canvas thread angle.

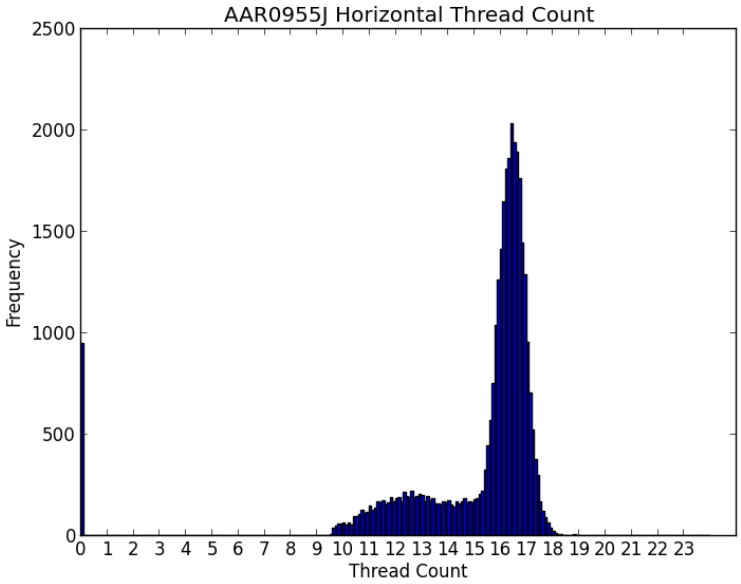

Plate 11.b Histogram of horizontal thread (in this case related to the warp) count readings.

Showing variation in thread count per centimetre.

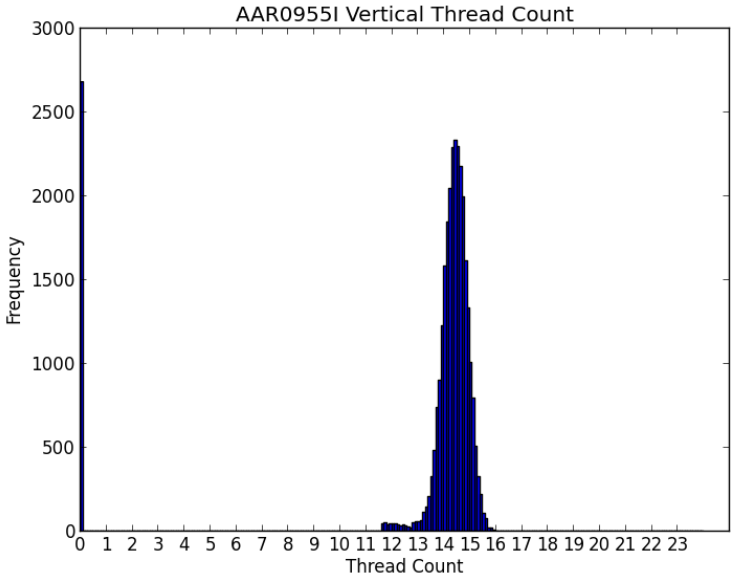

Plate 11.c Histogram of vertical thread count readings (in this case related to the weft).

Showing variation in thread count per centimetre.

Plate 11.d Table of thread count data (threads per centimetre)

	Mean	Estimated thread count (mode)
Warp (horizontal)	14.7	14.7
Weft(vertical)	14.41	14.4

Plate 12. Detail, bottom right corner, inscription ‘M[L]’ (in Cyrillic).

Plate 13. Detail, upper left corner showing ground and paint ending at tacking margins.

Plate 14.a Detail of canvas, lower tacking margin.

The canvas is a simple tabby weave. The fibre a bast type, probably linen.

Plate 14.b Detail of canvas edge, lower tacking margin, selvedge edge.

The ground and paint layers overlap the turnover edge slightly.

Plate 14.c Detail of the tacking margin, left.

The stress crack in the brittle paint at the turn over edge is visible.

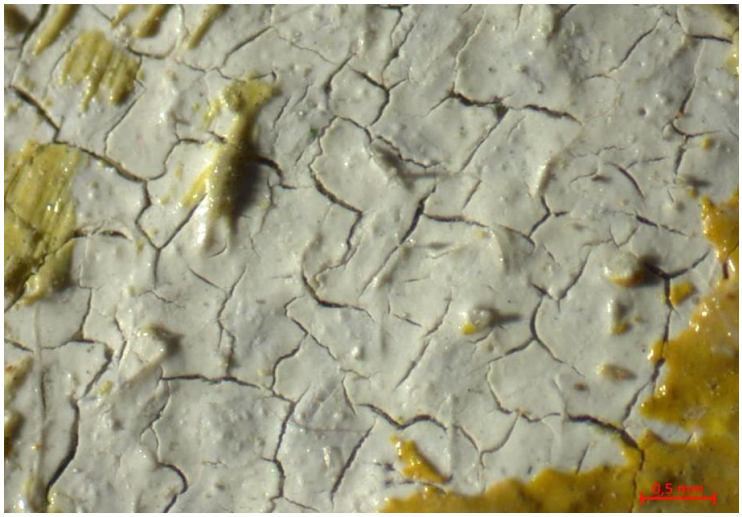

Plate 15.a Macro detail of ground, recto, showing the characteristic crack pattern.

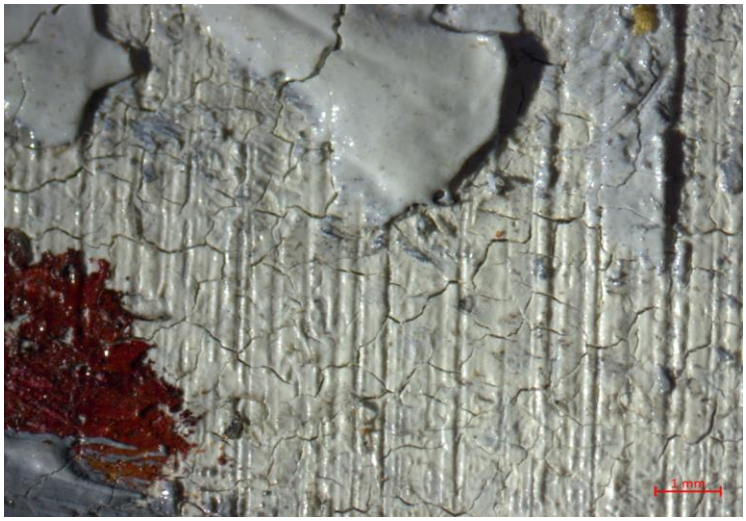

Plate 15.b Detail ground and paint.

Showing the very different craquelure of the paint, which passes over cracks in the ground, and the brush strokes visible in the ground.

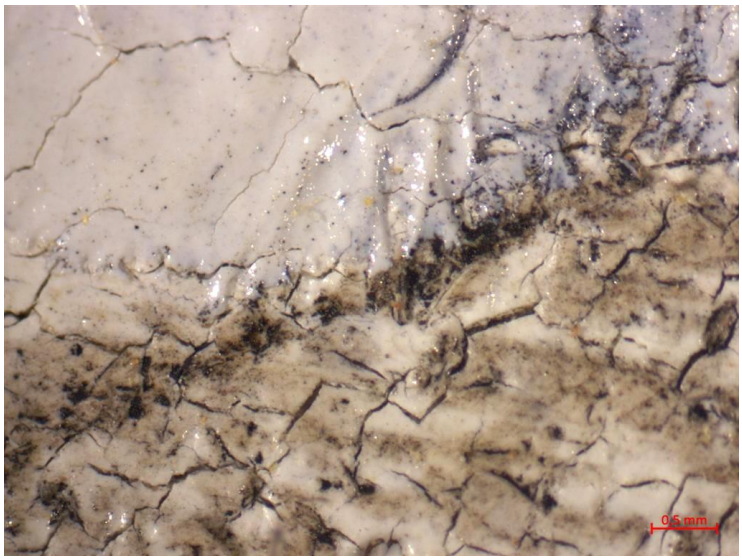

Plate 15.c Detail of ground and underdrawing.

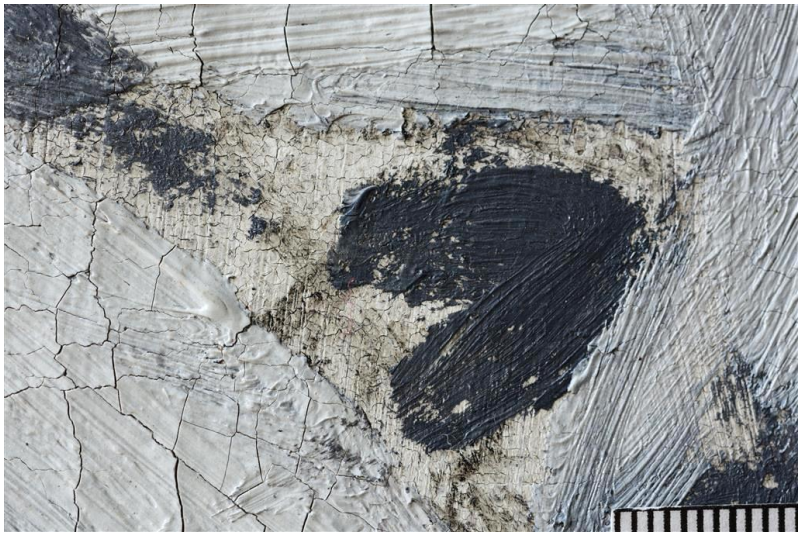

Plate 16.a Detail of canvas edge from verso, showing multiple layers of canvas and lining.

Plate 16.b Detail of painted surface, recto, showing the brushy grey lines around the painted forms.

Plate 16.c Detail of the lobster, oblique illumination, showing impasto in the whites.

Plate 17.a Detail of verso, showing paint and overlying white layer.

The strip to the left edge has not been painted over.

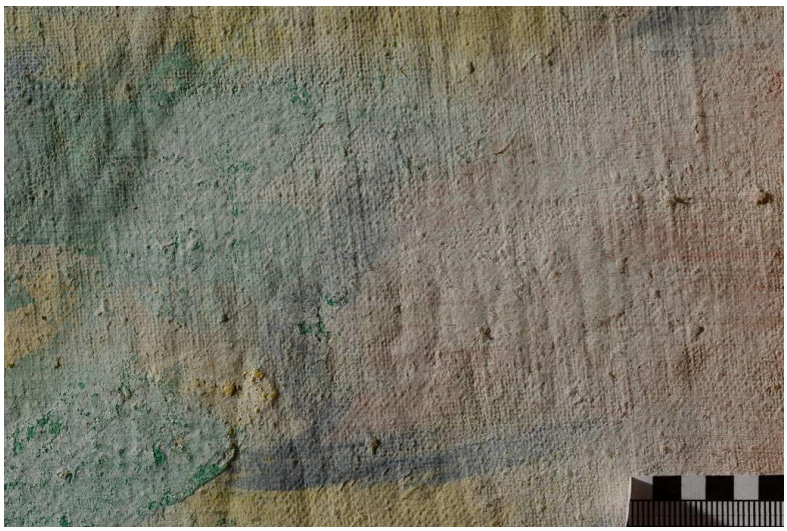

Plate 17.b Detail of verso, showing paint and overlying white layer.

The surface deformation caused by the presence of heavily painted areas on the verso is visible, as are slubby thread inclusions in the canvas.

Plate 17.c Detail of upper tacking edge, showing that the paint on the verso extends to the present cut edge.

Plate 18. Image showing approximate location of samples taken for materials analysis, recto.

Plate 19. Image showing approximate location of samples taken for materials analysis, verso.

App.5 Cross-sections[38]

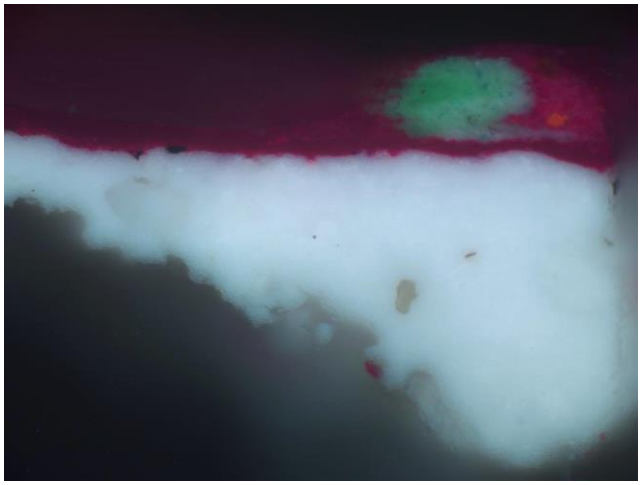

a.

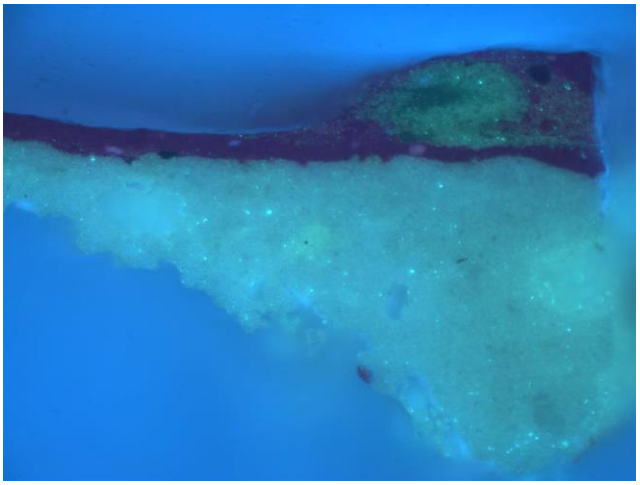

b.

Plate 20. Cross-section, Sample [14], recto.

Image ~260µm high. Pink from background decoration. The white ground includes particles displaying the green luminescence characteristic of zinc white under UV illumination. An area of green paint is mixed into the pink paint layer.

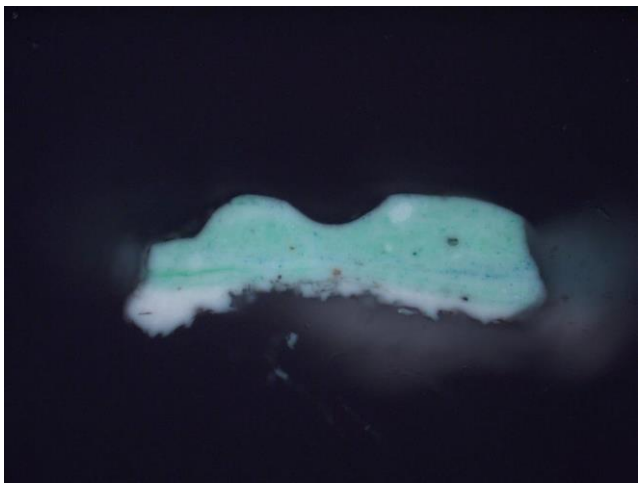

a.

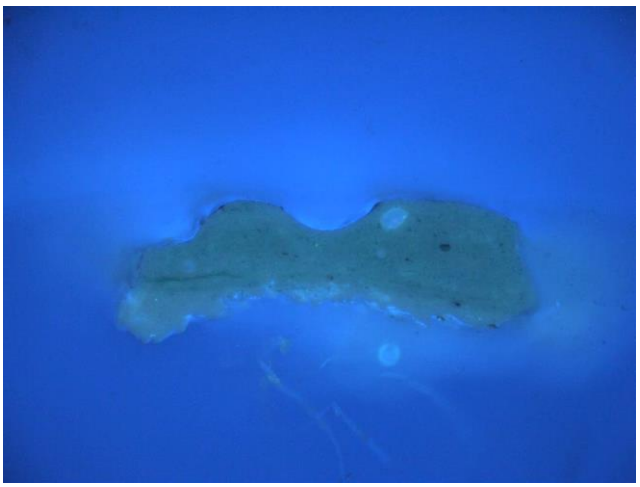

b.

Plate 21. Cross-section, Sample [15], recto.

Image ~1mm high. Green from background decoration. A small amount of material displaying a bluish luminescence in UV can be seen at the base of the sample, possibly from a canvas size layer. The green paint appears to be incompletely mixed, with horizontal streaks of darker green and blue.

[38] Photographed under visible light, left (**a.**), and with ultraviolet illumination, right (**b.**), unless otherwise stated.

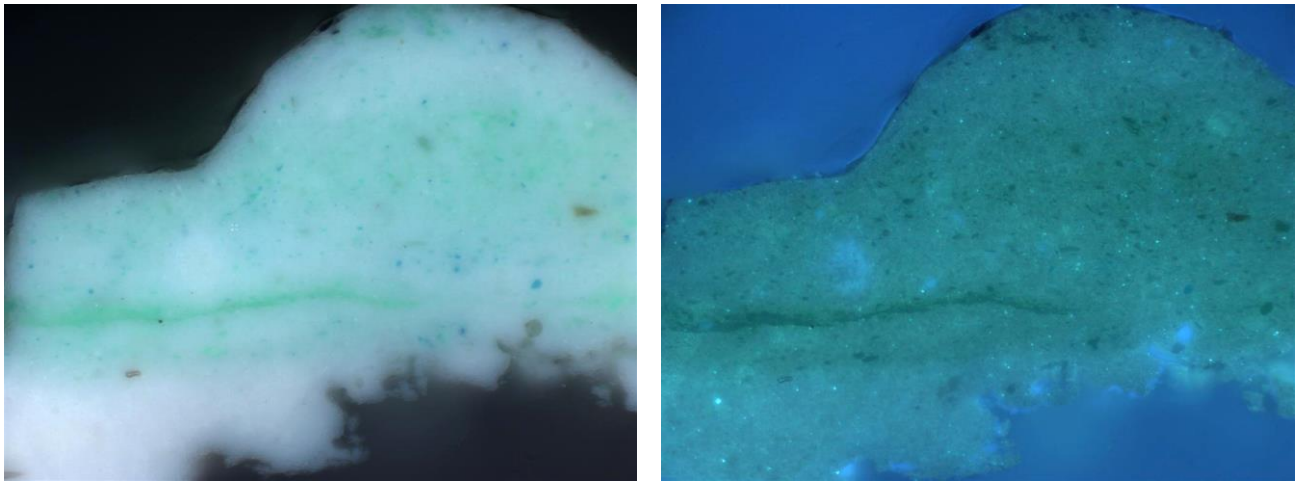

a. **b.**

Plate 22. Cross-section, Sample [15], recto.

Image ~260µm high. Green from background decoration, detail at higher magnification, showing the dark green streak at the left-hand side, and areas of white and blue particles.

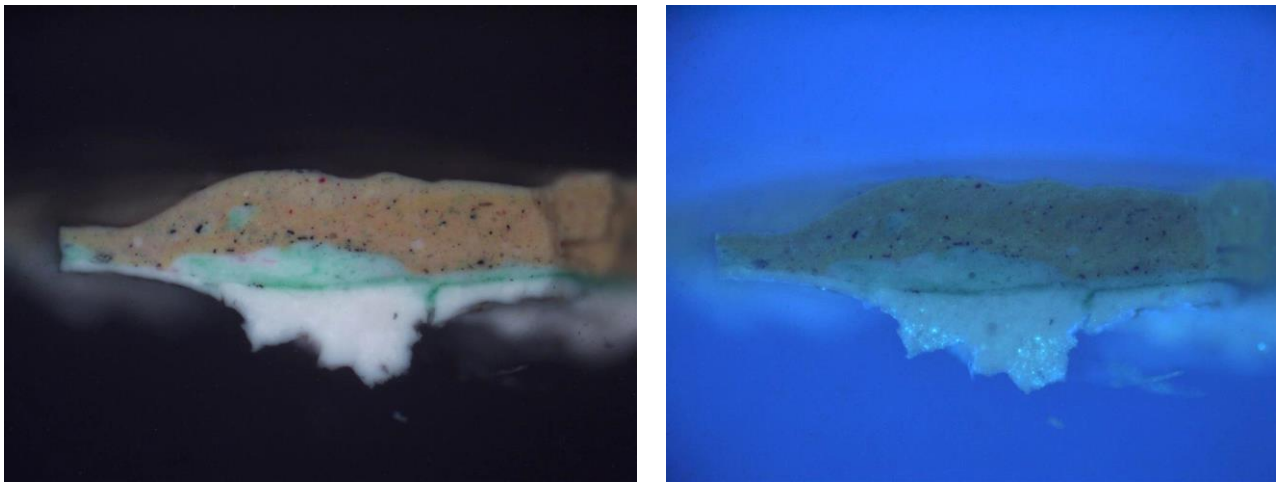

a. **b.**

Plate 23. Cross-section, Sample [17], recto.

Image ~1mm high. Dull grey yellow from table. The white ground layer includes particles with the green luminescence characteristic of zinc white, but these appear to be much more concentrated in the lower part of the layer. An inhomogeneous green layer lies on top of the ground, with a darker green streak at the base, and also streaks of pink. The yellow-brown layer includes black, red and green particles and has a light green region in one area, probably paint from the layer below.

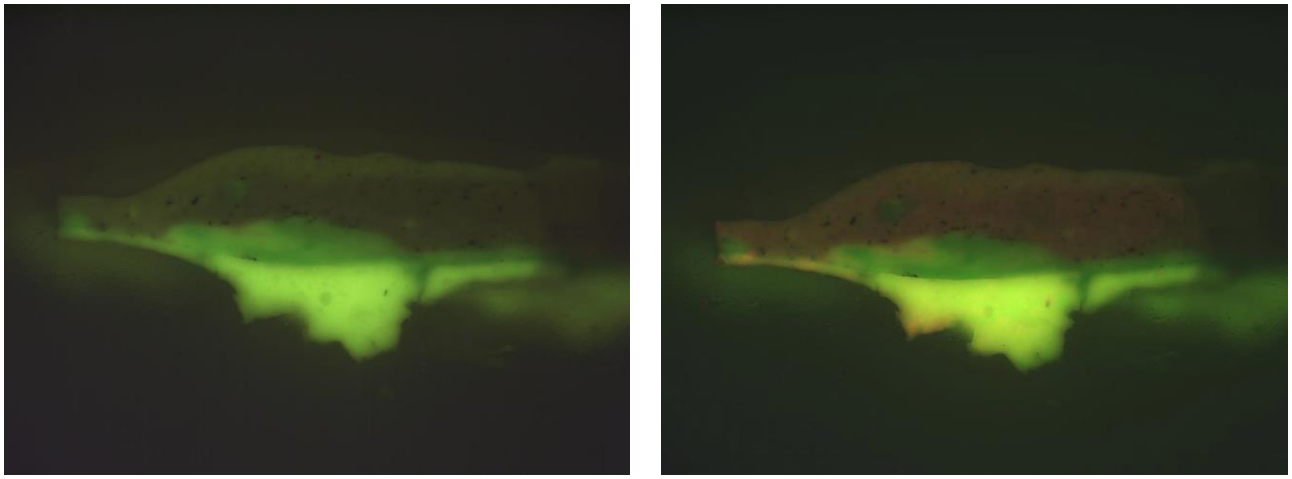

a. **b.**

Plate 24. Cross-section, Sample [17], recto, stained with SYPRO® Ruby.

Image ~1mm high viewed with Leica I3 filter before (left) and after (right) staining. A very faint pink coloration in the ground layer suggests the presence of protein, with stronger pink staining visible in the left-hand outer edge of the layer. There is also clear pink staining of yellow-grey layer, although the green layer appears unchanged.

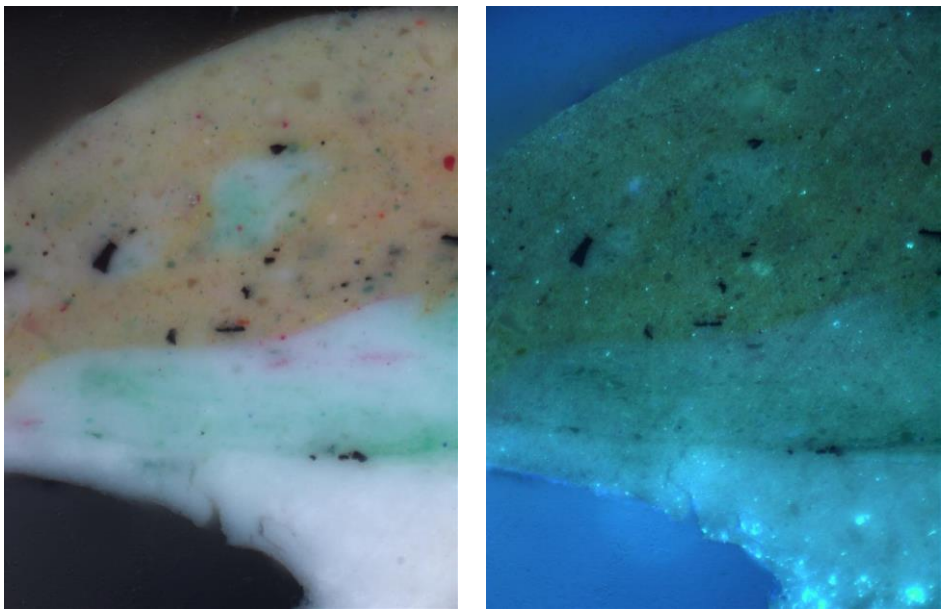

a. **b.**

Plate 25. Cross-section, Sample [17], recto.

Image ~260µm high. Dull grey yellow from table, detail at higher magnification, showing more clearly the mix of coloured particles in the paint layers.

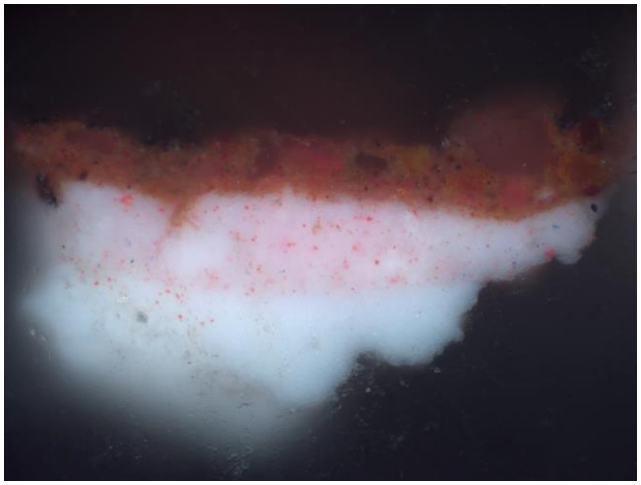

a.

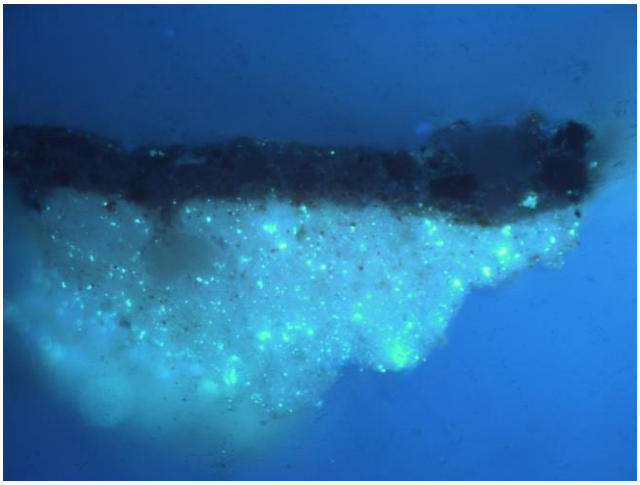

b.

Plate 26. Cross-section, Sample [22], verso.

Image ~260µm high. Brown from the verso. White ground covered with a pale pink layer including fine red particles and a few blue particles. Both layers contain many UV-luminescent particles with the characteristic appearance of zinc white. The uppermost orange-brown layer has orange-red, brown and colourless particles.

a.

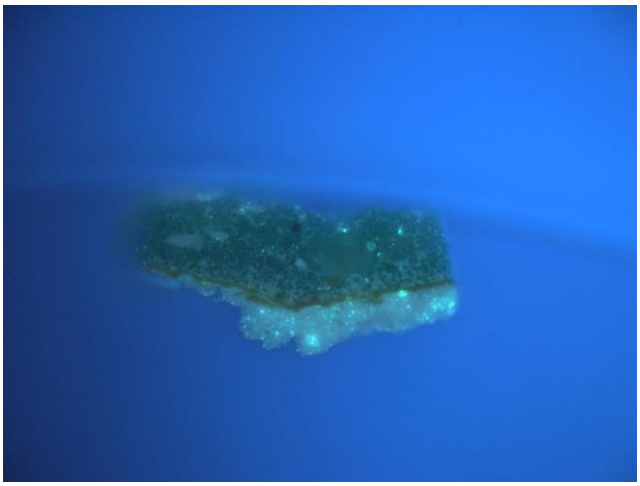

b.

Plate 27. Cross-section, Sample [23], verso.

Image ~1mm high. Green from the verso. As in sample 22, the ground contains numerous luminescent particles. This is covered with a fairly thin yellow paint layer, then a thick bright green layer including some areas of white.

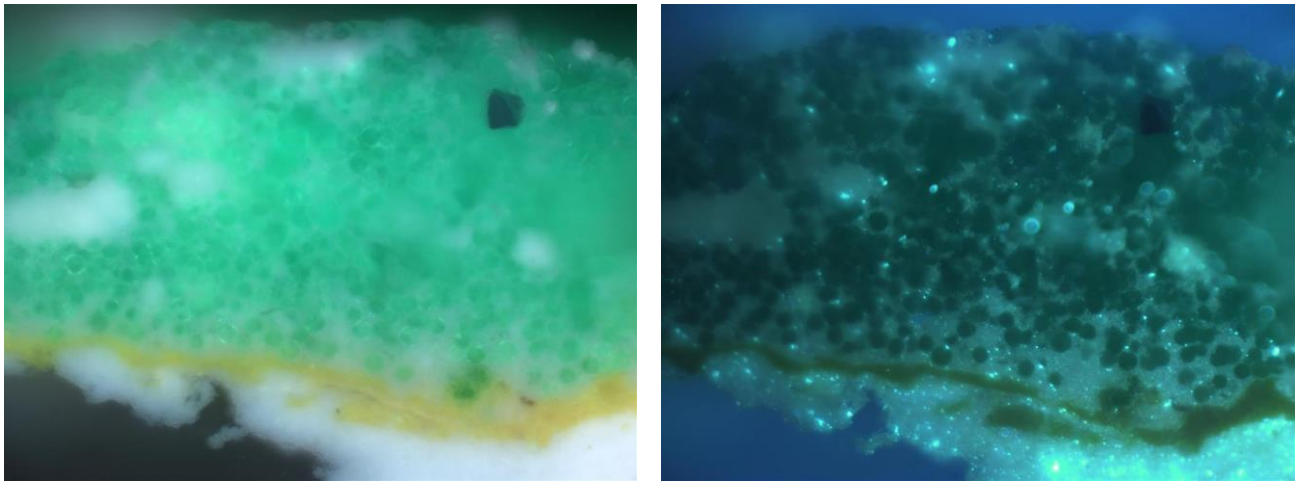

a. **b.**

Plate 28. Cross-section, Sample [23], verso.

Image ~260µm high. Green from the verso, detail at increased magnification, showing the distinctive rounded particles of emerald green in the bright green paint.